Received: 22 September 2023 | Revised: 4 May 2024 | Accepted: 22 June 2024

DOI: 10.1002/rnc.7517

RESEARCH ARTICLE

WILEY

Adaptive finite-time tracking control of nonlinear systems subject to input hysteresis and multiple objective constraints

Wei Zhao[1,2,3] | **Yu-Qun Han**[1,2,3] | **Ya-Feng Zhou**[1,2,3] | **Shan-Liang Zhu**[1,2,3]

[1]School of Mathematics and Physics, Qingdao University of Science and Technology, Qingdao, China

[2]The Research Institute for Mathematics and Interdisciplinary Sciences, Qingdao University of Science and Technology, Qingdao, China

[3]Qingdao Innovation Center of Artificial Intelligence Ocean Technology, Qingdao University of Science and Technology, Qingdao, China

Correspondence
Shan-Liang Zhu, School of Mathematics and Physics, Qingdao University of Science and Technology, Qingdao 266061, China.
Email: zhushanliang@qust.edu.cn

Abstract

In this article, the problem of adaptive finite-time tracking control for a class of nonlinear systems subject to backlash-like input hysteresis and multiple objective constraints is investigated. For the purpose of realizing multiple objective constraints, a new time-varying barrier function (TVBF) is introduced to ensure that all objective constraint functions are always within the defined range. Meanwhile, based on the combination of the command filter approach and adaptive backstepping control, an error compensation system (ECS) is supplied to reduce the impact of filter error on control performance. Additionally, the problem of "singularity" caused by hysteresis is avoided by linearizing the backlash-like hysteresis model, and Nussbaum-type function is also applied to reduce the influence of hysteresis on the stability of the system. Then, by combining multi-dimensional Taylor network (MTN) technology and command filter backstepping approach, an adaptive finite-time control strategy is designed. The proposed control strategy ensures that all the signals in the closed-loop system realize finite-time semi-globally uniformly ultimately bounded (SGUUB), and the output signal of the system can track the reference signal greatly while adhering to multiple objective constraints. Finally, the effectiveness of the proposed control strategy is verified by a practical simulation example.

KEYWORDS

adaptive finite-time control, backlash-like hysteresis, multi-dimensional Taylor network, multiple objective constraints, nonlinear systems

1 | INTRODUCTION

In practical industrial processes, a plethora of complex nonlinear systems prevail. Therefore, how to deal with the nonlinear characteristics of the nonlinear systems and control the systems effectively has been paid much attention. To solve these problems, various control methods have been proposed, such as adaptive backstepping control,[1,2] sliding mode control,[3] robust control[4] and fault-tolerant control.[5] In recent decades, adaptive backstepping control has been widely used in various nonlinear systems, such as large-scale systems,[6] nonstrict-feedback systems,[7,8] switched systems[9] and strict-feedback high-order nonlinear systems.[10,11] In particular, many control strategies proposed by combining fuzzy logic systems (FLSs) and neural networks (NNs) with adaptive backstepping control have been used to control various

nonlinear systems due to their optimal approximation properties.[12–16] It is important to note that MTN, as a kind of NNs, has been widely applied to the design of adaptive controllers.[17–19] However, in the design of adaptive backstepping control schemes, there exists a problem of "complexity explosion" due to the repeated differentiation of the virtual control signal. To address this issue, the dynamic surface control (DSC) method was proposed,[20–22] which introduces a first-order differential filter for the virtual control signal at each step of the controller design. However, this method overlooks the potential problem that filter error may compromise control performance. Therefore, once the command filter method[23,24] was introduced, it became a significant breakthrough in the field of nonlinear system control. It not only overcomes the problem of "complexity explosion", but also compensates for the filter error by introducing an error compensation system(ECS). Subsequently, it has been widely applied to control nonlinear systems, such as switched systems,[25] large-scale systems[26] and multi-agent systems.[27] In addition, in many practical applications, it is often necessary to ensure that control target is achieved within a finite time in order to improve control accuracy, convergence rate and anti-interference performance. Therefore, integrating DSC method or the command filter method with finite-time control has become a considerably practical approach.[28–30] However, none of the above works considers the constraint problem for nonlinear systems.

In reality, real systems often encounter various types of constraints. When the system violates constraints, it may exhibit problems, such as performance degradation and system instability. Therefore, constraint problem has always been an important research direction in system stability control. Currently, there have been numerous control methods proposed to address it, among which barrier Lyapunov functions (BLFs) method[31–33] is the most commonly used one. By using the constrained properties of BLFs with different structures, the system states can be effectively maintained within the defined limits, so as to solve the constrained control problem. An adaptive finite-time control scheme based on command filter method was proposed in[34] by using log-type BLFs to solve the output constraint problem. However, as a generalization of output constraints, multiple objective constraints have received little attention. For most practical systems, multiple objective constraints are unavoidable. For instance, in industrial production processes, we may need to simultaneously consider production efficiency, quality control, and cost control objectives. By representing these objectives as constraints, the optimal trade-off solutions can be developed by utilizing optimization techniques. Additionally, in transportation planning, constraints need to be considered simultaneously such as road capacity, traffic flow and road safety to develop optimal traffic routes and planning strategies. Therefore, it is of great practical significance to realize effective control of multiple objective constrained systems.

In addition, hysteresis is also an inevitable factor affecting the control accuracy of the system. Consequently, how to reduce the impact of hysteresis on system stability and improve the control effect has been an important research topic.[35–37] For nonlinear systems with backlash-like hysteresis, authors in Reference 36 linearized hysteresis model to deal with input hysteresis, which effectively improved the adaptive control effect of the system. Different from Reference 36, authors in Reference 38 used Nussbaum-type function to deal with Bouc-Wen hysteresis of the switched systems. However, the aforementioned work has ignored the impact of multiple objective constraints on system stability.

It is worth noting that in many practical engineering systems, it is common for multiple objective constraints and input hysteresis to exist simultaneously. Therefore, it is of profound research significance to explore how to address this issue within the framework of finite-time control. In light of this, an adaptive finite-time tracking control scheme based on command filter method is proposed for nonlinear systems with backlash-like input hysteresis and multiple objective constraints. Firstly, a novel TVBF is introduced to solve the multiple objective constraints problem. Secondly, the DSC technique is combined with the adaptive backstepping method to avoid the "complexity explosion" problem. At the same time, an ECS is utilized to reduce the filter error. In addition, the backlash-like hysteresis model is used to transform the hysteresis nonlinearity into linear combination terms with bounded error to avoid the "singularity" problem, and the Nussbaum-type function is supplied to reduce the influence of hysteresis on system stability. In each of backstepping design process, one MTN is used to approximate unknown nonlinearities in the system. Finally, an adaptive finite-time control strategy based on command filter method is proposed. Compared with the existing research work, the main contributions of this article are as follows:

(1) This article presents a novel application of MTN approximation technique to control nonlinear systems that are simultaneously subjected to multiple objective constraints and backlash-like input hysteresis. Despite the wide range of applications of MTN in nonlinear systems,[9,39,40] its extension to the control of nonlinear systems under the combined influence of multiple objective constraints and input hysteresis effects has been lacking. This article fills the gap in the application of the MTN technique in this particular field.
(2) In this article, a new finite-time command filter constraint control scheme is introduced for nonlinear systems. Different from the traditional finite-time control method adopted in References 41 and 42, this article designs a novel

DSC-based finite-time control scheme, and introduces an improved ECS to reduce the filter error. This scheme effectively solves the problem of "complexity explosion" caused by repeated differentiation of virtual control signals and comprehensively considers the influence of multiple objective constraints and hysteresis input on the stability of the system which improves the control performance to a great extent.

(3) Unlike,[36] this article not only linearizes the backlash-like hysteresis model to handle the hysteresis nonlinearity which avoids the "singularity" problem but also utilizes Nussbaum-type function to mitigate the impact of hysteresis on the stability of the system. Ultimately, a MTN-based adaptive finite-time control scheme is designed, which ensures that all signals in the closed-loop systems achieve finite-time semi-globally uniformly ultimately bounded (SGUUB).

2 | PROBLEM DESCRIPTION AND PRELIMINARY KNOWLEDGE

2.1 | Problem description

This article considers the following nonlinear system with unknown input hysteresis:

$$\begin{cases} \dot{x}_i = x_{i+1} + \sigma_i(\bar{\boldsymbol{x}}_i) + \phi_i(\bar{\boldsymbol{x}}_i, t), \\ i = 1, \ldots, n-1, \\ \dot{x}_n = u(v) + \sigma_n(\bar{\boldsymbol{x}}_n) + \phi_n(\bar{\boldsymbol{x}}_n, t), \\ y = x_1, \end{cases} \tag{1}$$

where $\bar{\boldsymbol{x}}_n = [x_1, \ldots, x_n]^{\mathrm{T}} \in R^n$ represents the state vector with $\bar{\boldsymbol{x}}_i = [x_1, \ldots, x_i]^{\mathrm{T}} \in R^i$, for $i = 1, \ldots, n-1$; $y \in R$ represents the output of the controlled system. The states of the nonlinear systems (1) considered in this article are all measurable. $\sigma_i : R^i \to R$ denotes unknown function with $\sigma_i(0) = 0$. ϕ_i is defined as the unknown but bounded external time-varying disturbance. u and v are the system output and the input of the backlash-like hysteresis, respectively. In order to address the influence of hysteresis on system stability, the following hysteresis model is introduced to characterize the nonlinear hysteresis behavior:

$$\frac{du}{dt} = \overline{\psi}\left|\frac{dv}{dt}\right|(\ell v - u) + \mathfrak{F}\frac{dv}{dt}, \tag{2}$$

where $\overline{\psi}$, ℓ, $\mathfrak{F}$ are unknown constants with $\ell > \mathfrak{F}$.

According to References 36 and 43, (2) can be transformed into the following linear combination

$$u(t) = \ell v(t) + \wp(v) \tag{3}$$

with the specific expression of $\wp(v)$ as follows

$$\wp(v) = [u_0 - \ell v_0]e^{\overline{\psi}(v-v_0)\mathrm{sgn}\dot{v}} + e^{-\overline{\psi}v\mathrm{sgn}\dot{v}}\int_{v_0}^{v}[\mathfrak{F} - \ell]e^{\overline{\psi}\xi\mathrm{sgn}\dot{v}}d\xi, \tag{4}$$

where u_0 and v_0 are the initial value of u and v, respectively. Meanwhile, $\wp(v)$ is bounded, satisfying

$$|\wp(v)| \le \overline{\wp}, \tag{5}$$

where $\overline{\wp} > 0$ is the upper bound of $\wp(v)$.

Remark 1. Figure 1 shows the image of hysteresis model (2) when k takes different values, where $\overline{\psi} = 1$, $\ell = 3$, $\mathfrak{F} = 0.4$. Hysteresis input is $v(t) = ksin(2.5t)$, where $k = 6.5$, $k = 4.5$, $k = 2.5$, respectively.

For the reference signal y_r, this article is to design a control strategy to achieve the following goals:

(i) All signals in the closed-loop systems achieve SGUUB in finite time.

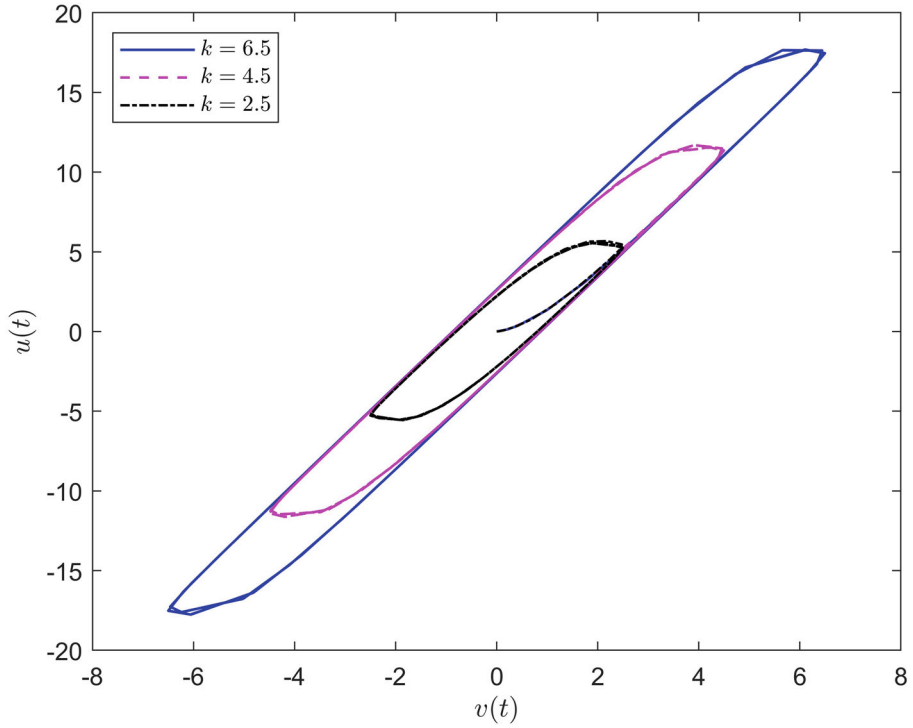

FIGURE 1 Hysteresis curves.

(ii) The tracking error approaches an arbitrarily small neighborhood of the origin in finite time.
(iii) Multiple objective constraints are achieved, that is, $-b_{\varsigma_1}(t) < I_i(x_1) < b_{\varsigma_2}(t)$ are satisfied at the same time, where $b_{\varsigma_1}(t)$ and $b_{\varsigma_2}(t)$ are asymmetric and time-varying constraint functions. $I_i(x_1) = \bar{s}_{k1}x_1 + \bar{s}_{k2}x_1^2 + \cdots + \bar{s}_{ki}x_1^i$ mean different objective functions. The selection of $\bar{s}_{ki}(i, k = 1, 2, \ldots, M)$ needs to ensure that every objective function is within the asymmetric constraint range.

2.2 | Assumptions, Definitions, and Lemmas

In order to facilitate the design of the controller, the following Assumptions, Definitions and Lemmas are given.

Assumption 1 (44). The reference signal y_r and its ith time derivative $y_r^{(i)}$ are continuous and bounded, $i = 1, \ldots, n$. Therefore, there exist some constants $\overline{\mu}_1, \overline{\mu}_2, \mu_1, \ldots, \mu_n > 0$ such that $-\overline{\mu}_1 \le y_r \le \overline{\mu}_2$, $|\dot{y}_r| < \mu_1, \ldots, \left|y_r^{(n)}\right| < \mu_n, \forall t > 0$.

Remark 2. It is worth noting that Assumption 1 is a normal assumption for nonlinear systems which can be found in existing work.[44–46]

Definition 1 (47). Any continuous functions $N(\chi)$ is said to be a Nussbaum-type function if it has the following properties:

$$\lim_{\xi\to\infty} \sup \frac{1}{\xi}\int_0^{\xi} N(\chi)d\chi = +\infty, \tag{6}$$

$$\lim_{\xi\to\infty} \inf \frac{1}{\xi}\int_0^{\xi} N(\chi)d\chi = -\infty. \tag{7}$$

It is important to note that many continuous functions can serve as a Nussbaum-type function, such as $\chi^2\cos(\chi)$, $e^{\chi^2}\cos\left(\frac{\pi}{2\chi}\right)$.

Lemma 1 (47). *Let $V(\cdot)$ and $\chi(\cdot)$ be smooth functions defined on $[0, t_f)$ with $V(t) \geq 0, \forall t \in [0, t_f)$. $N(\cdot)$ is an even smooth Nussbaum-type function and ρ_0 is a nonzero constant. If the following inequality holds*

$$V(t) \leq \int_0^t (\rho_0 N(\chi) + 1)\dot{\chi} d\tau + \rho_1, \forall t \in [0, t_f), \tag{8}$$

where ρ_1 is a suitable constant, then $V(t)$, $\chi(t)$ and $\int_0^t (\rho_0 N(\chi) + 1)\dot{\chi} d\tau$ are bounded on $[0, t_f)$.

Lemma 2 (48). *The nonlinear system $\dot{x} = f(x)$ is practically finite-time stable if there exists a smooth positive definite function V such that $\dot{V} \leq -\eta_1 V - \eta_2 V^{\hbar} + \iota, \forall t \in T$, where the setting time T_r is given as $T_r \leq \max\left\{ t_0 + \frac{1}{\theta_0 \eta_1 (1-\hbar)} \ln \frac{\theta_0 \eta_1 V^{(1-\hbar)}(t_0) + \eta_2}{\eta_2}, t_0 + \frac{1}{\eta_1 (1-\hbar)} \ln \frac{\eta_1 V^{(1-\hbar)}(t_0) + \theta_0 \eta_2}{\theta_0 \eta_2} \right\}$ with $\eta_1 > 0, \eta_2 > 0, \iota \in (0, \infty), 0 < \hbar < 1, 0 < \theta_0 < 1$.*

Remark 3. Apparently, the tracking error cannot converge to zero, but larger η_1 and η_2 can be used to ensure that the tracking error is small enough within a finite time T_r, and the setting time T_r also can be accurately estimated.

Lemma 3 (49). *For any constants $\alpha > 0$, $\beta > 0$ and real valued function $\varpi(X, Y)$, the following inequality holds*

$$|X|^{\alpha} |Y|^{\beta} \leq \frac{\alpha \varpi(X, Y) |X|^{\alpha+\beta}}{\alpha + \beta} + \frac{\beta \varpi(X, Y)^{-\frac{\alpha}{\beta}} |Y|^{\alpha+\beta}}{\alpha + \beta}. \tag{9}$$

Lemma 4 (Young's inequality[50]). *For $\forall(\varphi_1, y) \in R^2$ and $\forall \Delta > 0$, the following inequality holds*

$$\varphi_1 y \leq \frac{\Delta^a}{a} |\varphi_1|^a + \frac{1}{b\Delta^b} |y|^b, \tag{10}$$

where $a > 1$ and $b > 1$ with $(a-1)(b-1) = 1$.

Lemma 5 (51). *For $h_i \in R, i = 1, \ldots, N, 0 < \tilde{p} \leq 1$, the following inequality holds*

$$\left(\sum_{i=1}^{N} |h_i| \right)^{\tilde{p}} \leq \sum_{i=1}^{N} |h_i|^{\tilde{p}} \leq N^{1-\tilde{p}} \left(\sum_{i=1}^{N} |h_i| \right)^{\tilde{p}}. \tag{11}$$

2.3 | Multi-dimensional Taylor network

In this article, MTNs will be used to approximate unknown nonlinearities that arise during the controller design process. Further information about MTNs can be found in the work of References 40,52,53. However, for the sake of brevity, only the following approximation property of MTN is presented in this article, as stated in Lemma 6.

Lemma 6 (40,52,53). *If $f(\boldsymbol{z})$ is a continuous and unknown function defined on the compact set Ω_z, then, there exists a MTN used to estimate $f(\boldsymbol{z})$ for $\forall \bar{\varepsilon} > 0$ such that*

$$f(\boldsymbol{z}) = \lambda^{\mathrm{T}} P_{m_n}(\boldsymbol{z}) + \varepsilon(\boldsymbol{z}), \tag{12}$$

where $P_{m_n}(\boldsymbol{z}) = \left[z_1, \ldots, z_n, z_1^2, z_1 z_2, \ldots, z_n^2, \ldots, z_1^m, z_1^{m-1} z_2, \ldots, z_n^m \right]^{\mathrm{T}} \in R^l$ represents the middle intermediate input layer of MTN. $\boldsymbol{z} = [z_1, z_2, \ldots, z_n]^{\mathrm{T}} \in R^n$ and $\lambda = [\theta_1, \theta_2, \ldots, \theta_l]^{\mathrm{T}} \in R^l$ are the input vector and the weight vector of MTN, respectively. $\varepsilon(\boldsymbol{z})$ denotes the error generated in the estimation with $|\varepsilon(\boldsymbol{z})| \leq \bar{\varepsilon}$.

3 | MAIN RESULTS

This section includes two aspects: the design process of adaptive controller via backstepping method and stability analysis of the closed-loop system.

Firstly, in order to achieve multiple objective constraints, the following asymmetric TVBF is introduced, whose expression is as follows

$$p = \frac{I + b_{c_1}}{I + b_{\varsigma_1}(t)} - \frac{I - b_{c_2}}{I - b_{\varsigma_2}(t)}, \tag{13}$$

where $b_{c_1} > 0$ and $b_{c_2} > 0$ are the design parameters and satisfying $b_{c_1} < b_{\varsigma_1}$, $b_{c_2} < b_{\varsigma_2}$. $b_{\varsigma_1}(t)$, $b_{\varsigma_2}(t)$ are asymmetric and time-varying constraint functions. I is defined in the open region Ω and its initial value $I(0)$ is also in the region Ω.

Remark 4. Multiple objective constraints means that different $I_i(x_1) = \bar{s}_{k1}x_1 + \bar{s}_{k2}x_1^2 + \cdots + \bar{s}_{ki}x_1^i$ satisfies $-b_{\varsigma_1}(t) < I_i(x_1) < b_{\varsigma_2}(t)$ at the same time, where $\bar{s}_{ki}(i, k = 1, 2, \ldots, M)$ are the weighting coefficients and $M > 0$ is a positive integer. For the convenience of discussion, we use p and I to stand for the general form instead of p_i and I_i, respectively. And it is worth stating that each I_i corresponds to each p_i in one-to-one correspondence. If $I \to (-b_{\varsigma_1})^+$ or $I \to b_{\varsigma_2}^-$, p approaches infinity. In brief, as long as p is guaranteed to be bounded, I also obeys the constraints. Therefore, the problem of satisfying the multiple objective constraints is transformed into ensuring the barrier function p bounded.

Remark 5. If and only if $I = x_1$, multiple objective constraints will be transformed into output constraint, which universally exist in constraint research. Therefore, the output constraint is just a special form of multiple objective constraints.

By taking derivative of p, it yields

$$\dot{p} = \tau_1 \dot{I} + \tau_2 = \tau_{11}\dot{x}_1 + \tau_2, \tag{14}$$

where $\tau_1 = \frac{b_{\varsigma_1}(t) - b_{c_1}}{[I + b_{\varsigma_1}(t)]^2} + \frac{b_{\varsigma_2}(t) - b_{c_2}}{[I - b_{\varsigma_2}(t)]^2}$, $\tau_2 = -\frac{(I + b_{c_1})\dot{b}_{\varsigma_1}(t)}{[I + b_{\varsigma_1}(t)]^2} + \frac{(b_{c_2} - I)\dot{b}_{\varsigma_2}(t)}{[I - b_{\varsigma_2}(t)]^2}$, $\tau_{11} = \tau_1 \frac{\partial I}{\partial x_1}$ and $\frac{\partial I}{\partial x_1} \neq 0$.

Therefore, the controller design in this article is based on the following coordinate transformation:

$$\begin{cases} z_1 = p - y_{r,c}, \\ z_i = x_i - x_{i,c}, \end{cases} \tag{15}$$

where $i = 2, \ldots, n$, $y_{r,c} = \frac{y_r + b_{c_1}}{y_r + b_{\varsigma_1}(t)} - \frac{y_r - b_{c_2}}{y_r - b_{\varsigma_2}(t)}$, y_r is the reference signal. $x_{i,c}$ is the output of the first-order filter, and the virtual control signal α_{i-1} is the input of the filter.

Remark 6. In this article, the command filter is introduced to solve the "complexity explosion" problem caused by the repeated differentiation of some nonlinear functions (such as virtual control signals) in the controller design process by using traditional adaptive backstepping method.[54,55] However, the command filter may produce filter errors that will further affect the control performance. Therefore, the error compensation signal $\varkappa_i$ is designed to eliminate the effect of the error $(x_{i,c} - \alpha_{i-1})$ in the filtering process.

Similar to References 51 and 56, the following ECS is introduced

$$\begin{cases} \dot{\varkappa}_1 = \tau_{11}(-k_1\varkappa_1 + x_{2,c} - \alpha_1 + \varkappa_2) - h_1\mathrm{sgn}(\varkappa_1), \\ \dot{\varkappa}_2 = -k_2\varkappa_2 + x_{3,c} - \alpha_2 + \varkappa_3 - h_2\mathrm{sgn}(\varkappa_2), \\ \dot{\varkappa}_i = -k_i\varkappa_i + x_{i+1,c} - \alpha_i - \varkappa_{i-1} + \varkappa_{i+1} - h_i\mathrm{sgn}(\varkappa_i), \\ i = 3, \ldots, n-1, \\ \dot{\varkappa}_n = -k_n\varkappa_n - \varkappa_{n-1} - h_n\mathrm{sgn}(\varkappa_n), \end{cases} \tag{16}$$

where $\varkappa_i(0) = 0$ is the initial value of the error compensation signal $\varkappa_i$. k_i and h_i both are positive design parameters, $\mathrm{sgn}(*)$ is sign function of $*$.

Furthermore, the compensated tracking error is defined as follows

$$\begin{aligned} w_1 &= z_1 - \varkappa_1, \\ w_i &= z_i - \varkappa_i, \quad i = 2, \ldots, n. \end{aligned} \tag{17}$$

Combining (15), (16), and (17), taking the derivative of w_i, the compensated tracking error can be rewritten as

$$\begin{cases} \dot{w}_1 = \tau_{11}(w_2 + \sigma_1 + \phi_1 + k_1\varkappa_1 + \alpha_1) + \tau_2 - \kappa_1\dot{y}_r + \kappa_2 + h_1\mathrm{sgn}(\varkappa_1), \\ \dot{w}_2 = w_3 + \sigma_2 + \phi_2 + k_2\varkappa_2 + \alpha_2 - \dot{x}_{2,c} + h_2\mathrm{sgn}(\varkappa_2), \\ \dot{w}_i = w_{i+1} + \sigma_i + \phi_i + k_i\varkappa_i + \alpha_i - \dot{x}_{i,c} + \varkappa_{i-1} + h_i\mathrm{sgn}(\varkappa_i), \\ \dot{w}_n = u(v) + \sigma_n + \phi_n + k_n\varkappa_n - \dot{x}_{n,c} + \varkappa_{n-1} + h_n\mathrm{sgn}(\varkappa_n), \end{cases} \tag{18}$$

where $\kappa_1 = \frac{b_{\varsigma_1}(t)-b_{c_1}}{[y_r+b_{\varsigma_1}(t)]^2} + \frac{b_{\varsigma_2}(t)-b_{c_2}}{[y_r-b_{\varsigma_2}(t)]^2}$, $\kappa_2 = \frac{(y_r+b_{c_1})\dot{b}_{\varsigma_1}(t)}{[y_r+b_{\varsigma_1}(t)]^2} - \frac{(b_{c_2}-y_r)\dot{b}_{\varsigma_2}(t)}{[y_r-b_{\varsigma_2}(t)]^2}$.

The detailed process of controller design is given below.

3.1 | Controller design

In this section, an adaptive MTN finite-time controller based on DSC technique is designed for nonlinear systems with input hysteresis and multiple objective constraints.

Step 1: Considering the first Lyapunov function V_1 as

$$V_1 = \frac{1}{2}w_1^2 + \frac{1}{2}\tilde{\theta}_1^2, \tag{19}$$

where $\theta_1 = \|\lambda_1\|^2$ denotes unknown constant, λ_1 is the weight vector of MTN. $\tilde{\theta}_1$ is the estimation error of θ_1 with $\tilde{\theta}_1 = \theta_1 - \hat{\theta}_1$, $\hat{\theta}_1$ is the estimation of θ_1.

In light of (18) and (19), the time derivative of V_1 is

$$\begin{aligned} \dot{V}_1 &= w_1\dot{w}_1 + \tilde{\theta}_1\dot{\tilde{\theta}}_1 \\ &= \tau_{11}w_1w_2 + \tau_{11}w_1(\sigma_1 + \phi_1 + k_1\varkappa_1 + \alpha_1) + w_1\tau_2 - \kappa_1w_1\dot{y}_r + \kappa_2w_1 + h_1w_1\mathrm{sgn}(\varkappa_1) - \tilde{\theta}_1\dot{\hat{\theta}}_1. \end{aligned} \tag{20}$$

Denoting $\varphi_1 = 1$ and $y = \tau_{11}w_1\phi_1$ along with taking $a = 2$, $b = 2$ and $\Delta = a_1$. Then, according to Lemma 4, (21) can be obtained as

$$\tau_{11}w_1\phi_1 \le \frac{1}{2}a_1^2 + \frac{1}{2a_1^2}\tau_{11}^2w_1^2\phi_1^2, \tag{21}$$

where $a_1 > 0$ is a constant.

Similarly, denoting $\varphi_1 = h_1$ and $y = \tau_{11}w_1\phi_1$ along with taking $a = 2$, $b = 2$ and $\Delta = 1$, then, according to Lemma 4, (22) can be obtained as

$$h_1w_1\mathrm{sgn}(\varkappa_1) \le \frac{1}{2}h_1^2 + \frac{1}{2}w_1^2, \tag{22}$$

Substituting (21) and (22) into (20), the time derivative of V_1 becomes

$$\dot{V}_1 \le \tau_{11}w_1(\alpha_1 + w_2 + k_1\varkappa_1) + w_1F_1 + \frac{1}{2}a_1^2 + \frac{1}{2}h_1^2 - \frac{1}{2}w_1^2 - \tilde{\theta}_1\dot{\hat{\theta}}_1, \tag{23}$$

where $F_1 = \tau_{11}\sigma_1 - \kappa_1\dot{y}_r + \kappa_2 + \tau_2 + \frac{1}{2a_1^2}\tau_{11}^2w_1\phi_1^2 + w_1$ is a combination of nonlinear functions.

Based on the MTN approximation technique in Lemma 5, for any constant $\bar{\varepsilon}_1 > 0$, F_1 can be approximated by a MTN, that is, the following formula is established

$$F_1 = \lambda_1^{\mathrm{T}}P_{m_1}(\boldsymbol{z}_1) + \varepsilon_1(\boldsymbol{z}_1), |\varepsilon_1(\boldsymbol{z}_1)| \le \bar{\varepsilon}_1, \tag{24}$$

where $\boldsymbol{z}_1 = [z_1]^{\mathrm{T}}$, $\varepsilon_1(\boldsymbol{z}_1)$ is the approximation error of the combination term F_1 and $\lambda_1^{\mathrm{T}}P_{m_1}$.

Furthermore, (25) can be obtained

$$w_1 F_1 \le w_1 \lambda_1^{\mathrm{T}} P_{m_1} + w_1 \bar{\varepsilon}_1, \tag{25}$$

Then, according to Lemma 4, (25) can be rewritten as

$$w_1 F_1 \le \frac{1}{2} l_1^2 + \frac{1}{2l_1^2} w_1^2 \theta_1 P_{m_1}^{\mathrm{T}} P_{m_1} + \frac{1}{2} w_1^2 + \frac{1}{2} \bar{\varepsilon}_1^2, \tag{26}$$

where $l_1 > 0$ is the constant.

Substituting (26) into (23) gives

$$\dot{V}_1 \le \tau_{11} w_1 (\alpha_1 + w_2 + k_1 \varkappa_1) + \frac{1}{2} a_1^2 + \frac{1}{2} l_1^2 + \frac{1}{2l_1^2} w_1^2 \theta_1 P_{m_1}^{\mathrm{T}} P_{m_1} + \frac{1}{2} \bar{\varepsilon}_1^2 + \frac{1}{2} h_1^2 - \tilde{\theta}_1 \dot{\hat{\theta}}_1. \tag{27}$$

Define the virtual control signal as follows

$$\alpha_1 = -k_1 z_1 - \frac{1}{2\tau_{11} l_1^2} w_1 \hat{\theta}_1 P_{m_1}^{\mathrm{T}} P_{m_1} - s_1 w_1^{\gamma}, \tag{28}$$

where $k_1 > 0$, $0 < \gamma \le 1$ and $s_1 > 0$ are all design parameters.

With the help of the virtual control signal α_1 and (26), the time derivative of V_1 becomes

$$\dot{V}_1 \le \tau_{11} w_1 w_2 - \tau_{11} k_1 w_1^2 - \tau_{11} s_1 w_1^{1+\gamma} + \frac{1}{2} \bar{\varepsilon}_1^2 + \frac{1}{2} a_1^2 + \frac{1}{2} h_1^2 + \frac{1}{2l_1^2} + \tilde{\theta}_1 \left(\frac{1}{2l_1^2} w_1^2 P_{m_1}^{\mathrm{T}} P_{m_1} - \dot{\hat{\theta}}_1 \right). \tag{29}$$

Step 2: Considering the second Lyapunov function V_2 as

$$V_2 = \frac{1}{2} w_2^2 + \frac{1}{2} \tilde{\theta}_2^2 + V_1, \tag{30}$$

where $\theta_2 = \|\lambda_2\|^2$ denotes unknown constant, λ_2 is the weight vector of MTN. $\tilde{\theta}_2$ is the estimation error of θ_2 with $\tilde{\theta}_2 = \theta_2 - \hat{\theta}_2$, $\hat{\theta}_2$ is the estimation of θ_2.

In light of (18) and (30), the time derivative of V_2 is

$$\dot{V}_2 = w_2 (w_3 + \sigma_2 + \phi_2 + k_2 \varkappa_2 + \alpha_2 - \dot{x}_{2,c}) + h_2 w_2 \mathrm{sgn}(\varkappa_2) - \tilde{\theta}_2 \dot{\hat{\theta}}_2 + \dot{V}_1. \tag{31}$$

According to Lemma 4, one has

$$w_2 \phi_2 \le \frac{1}{2} a_2^2 + \frac{1}{2a_2^2} w_2^2 \phi_2^2, \tag{32}$$

$$h_2 w_2 \mathrm{sgn}(\varkappa_2) \le \frac{1}{2} h_2^2 + \frac{1}{2} w_2^2, \tag{33}$$

where $a_2 > 0$ is a constant. Substituting (32) and (33) into (31), the time derivative of V_2 becomes

$$\dot{V}_2 \le w_2 (w_3 + k_2 \varkappa_2 + \alpha_2) - \tau_{11} w_1 w_2 + w_2 F_2 + \frac{1}{2} a_2^2 + \frac{1}{2} h_2^2 - \frac{1}{2} w_2^2 - \tilde{\theta}_2 \dot{\hat{\theta}}_2 + \dot{V}_1, \tag{34}$$

where $F_2 = \sigma_2 - \dot{x}_{2,c} + \frac{1}{2a_2^2} w_2 \phi_2^2 + \tau_{11} w_1 + w_2$ is a combination of nonlinear functions.

Based on the MTN approximation technique in Lemma 5, for any constant $\bar{\varepsilon}_2 > 0$, F_2 can be approximated by an MTN, that is, the following formula is established

$$F_2 = \lambda_2^{\mathrm{T}} P_{m_2}(\boldsymbol{z}_2) + \varepsilon_2(\boldsymbol{z}_2), |\varepsilon_2(\boldsymbol{z}_2)| \le \bar{\varepsilon}_2, \tag{35}$$

where $\boldsymbol{z}_2 = [z_1, z_2]^{\mathrm{T}}$, $\varepsilon_2(\boldsymbol{z}_2)$ is the approximation error of the combination term F_2 and $\lambda_2^{\mathrm{T}} P_{m_2}$.

Furthermore, (36) can be obtained

$$w_2F_2 \le w_2\lambda_2^{\mathrm{T}}P_{m_2} + w_2\bar{\varepsilon}_2. \tag{36}$$

Then, similar to (21) and (22), by rearranging Lemma 4, (36) can be rewritten as

$$w_2F_2 \le \frac{1}{2}l_2^2 + \frac{1}{2l_2^2}w_2^2\theta_2P_{m_2}^{\mathrm{T}}P_{m_2} + \frac{1}{2}w_2^2 + \frac{1}{2}\bar{\varepsilon}_2^2, \tag{37}$$

where $l_2 > 0$ is the constant.

Substituting (37) into (34) gives

$$\dot{V}_2 \le w_2(w_3 + k_2\varkappa_2 + \alpha_2) - \tau_{11}w_1w_2 + \frac{1}{2}l_2^2 + \frac{1}{2l_2^2}w_2^2\theta_2P_{m_2}^{\mathrm{T}}P_{m_2} + \frac{1}{2}\bar{\varepsilon}_2^2 + \frac{1}{2}a_2^2 + \frac{1}{2}h_2^2 - \tilde{\theta}_1\dot{\hat{\theta}}_1 + \dot{V}_1. \tag{38}$$

Define the virtual control signal as follows

$$\alpha_2 = -k_2z_2 - \frac{1}{2l_2^2}w_2\hat{\theta}_2P_{m_2}^{\mathrm{T}}P_{m_2} - s_2w_2^{\gamma}, \tag{39}$$

where $k_2 > 0$ is the constant, $0 < \gamma \le 1$ is the design parameter.

With the help of the virtual control signal α_2, (29) and (38), the time derivative of V_2 becomes

$$\dot{V}_2 \le w_2w_3 - \tau_{11}k_1w_1^2 - k_2w_2^2 - \tau_{11}s_1w_1^{1+\gamma} + \sum_{j=1}^{2}\left(\frac{1}{2}a_j^2 + \frac{1}{2}h_j^2 + \frac{1}{2}l_j^2 + \frac{1}{2}\bar{\varepsilon}_j^2\right) + \sum_{j=1}^{2}\tilde{\theta}_j\left(\frac{1}{2l_j^2}w_j^2P_{m_j}^{\mathrm{T}}P_{m_j} - \dot{\hat{\theta}}_j\right). \tag{40}$$

Step i: Considering the following Lyapunov function V_i as

$$V_i = \frac{1}{2}w_i^2 + \frac{1}{2}\tilde{\theta}_i^2 + V_{i-1}, \tag{41}$$

where $\theta_i = \|\lambda_i\|^2$ denotes unknown constant, λ_i is the weight vector of MTN. $\tilde{\theta}_i$ is the estimation error of θ_i with $\tilde{\theta}_i = \theta_i - \hat{\theta}_i$, $\hat{\theta}_i$ is the estimation of θ_i.

In light of (18) and (41), the time derivative of V_i is

$$\begin{aligned}\dot{V}_i &= w_i\dot{w}_i + \tilde{\theta}_i\dot{\tilde{\theta}}_i + \dot{V}_{i-1}\\ &= w_i(w_{i+1} + \sigma_i + \phi_i + k_i\varkappa_i + \alpha_i - \dot{x}_{i,c} + \varkappa_{i-1}) + h_iw_i\mathrm{sgn}(\varkappa_i) - \tilde{\theta}_i\dot{\hat{\theta}}_i + \dot{V}_{i-1}.\end{aligned} \tag{42}$$

Similar to (21) and (22), by rearranging Lemma 4, we have

$$w_i\phi_i \le \frac{1}{2}a_i^2 + \frac{1}{2a_i^2}w_i^2\phi_i^2, \tag{43}$$

$$h_iw_i\mathrm{sgn}(\varkappa_i) \le \frac{1}{2}h_i^2 + \frac{1}{2}w_i^2, \tag{44}$$

where $a_i > 0$ is a constant.

Substituting (43) and (44) into (42), the time derivative of V_i becomes

$$\dot{V}_i \le w_i(w_{i+1} + k_i\varkappa_i + \alpha_i - w_{i-1}) + w_iF_i + \frac{1}{2}a_i^2 + \frac{1}{2}h_i^2 - \frac{1}{2}w_i^2 - \tilde{\theta}_i\dot{\hat{\theta}}_i + \dot{V}_{i-1}, \tag{45}$$

where $F_i = \sigma_i - \dot{x}_{i,c} + \frac{1}{2a_i^2}w_i\phi_i^2 + w_i + z_{i-1}$ is a combination of nonlinear functions.

Based on the MTN approximation technique in Lemma 5, for any constant $\bar{\varepsilon}_i > 0$, F_i can be approximated by an MTN, that is, the following formula is established

$$F_i = \lambda_i^{\mathrm{T}} P_{m_i}(\boldsymbol{z}_i) + \varepsilon_i(\boldsymbol{z}_i), |\varepsilon_i(\boldsymbol{z}_i)| \leq \bar{\varepsilon}_i, \tag{46}$$

where $\boldsymbol{z}_i = [z_1, \ldots, z_i]^{\mathrm{T}}$, $\varepsilon_i(\boldsymbol{z}_i)$ is the approximation error of the combination term F_i and $\lambda_i^{\mathrm{T}} P_{m_i}$.

Furthermore, combining (45) and (46), (47) can be obtained

$$w_i F_i \leq w_i \lambda_i^{\mathrm{T}} P_{m_i} + w_i \bar{\varepsilon}_i. \tag{47}$$

Then, according Lemma 4, (47) can be rewritten as

$$w_i F_i \leq \frac{1}{2} l_i^2 + \frac{1}{2l_i^2} w_i^2 \theta_i P_{m_i}^{\mathrm{T}} P_{m_i} + \frac{1}{2} w_i^2 + \frac{1}{2} \bar{\varepsilon}_i^2, \tag{48}$$

where $l_i > 0$ is the constant.

Substituting (48) into (45) gives

$$\dot{V}_i \leq w_i(w_{i+1} + k_i \varkappa_i + \alpha_i - w_{i-1}) + \frac{1}{2} l_i^2 + \frac{1}{2l_i^2} w_i^2 \theta_i P_{m_i}^{\mathrm{T}} P_{m_i} + \frac{1}{2} \bar{\varepsilon}_i^2 + \frac{1}{2} a_i^2 + \frac{1}{2} h_i^2 - \tilde{\theta}_i \dot{\hat{\theta}}_i + \dot{V}_{i-1}. \tag{49}$$

Define the virtual control signal as follows

$$\alpha_i = -k_i z_i - \frac{1}{2l_i^2} w_i \hat{\theta}_i P_{m_i}^{\mathrm{T}} P_{m_i} - s_i w_i^{\gamma}, \tag{50}$$

where $k_i > 0$, $0 < \gamma \leq 1$, and $s_i > 0$ are all design parameters.

With the help of the virtual control signal α_i, (40) and (49), the time derivative of V_i becomes

$$\begin{aligned} \dot{V}_i \leq\ & w_i w_{i+1} - \tau_{11} s_1 w_1^{1+\gamma} - \sum_{j=2}^{i} s_j w_j^{1+\gamma} - \tau_{11} k_1 w_1^2 - \sum_{j=2}^{i} k_j w_j^2 \\ & + \sum_{j=1}^{i} \left(\frac{1}{2} a_j^2 + \frac{1}{2} h_j^2 + \frac{1}{2} l_j^2 + \frac{1}{2} \bar{\varepsilon}_j^2 \right) + \sum_{j=1}^{i} \tilde{\theta}_j \left(\frac{1}{2l_j^2} w_j^2 P_{m_j}^{\mathrm{T}} P_{m_j} - \dot{\hat{\theta}}_j \right). \end{aligned} \tag{51}$$

Step n: Considering the following Lyapunov function V_n as

$$V_n = \frac{1}{2} w_n^2 + \frac{1}{2} \tilde{\theta}_n^2 + V_{n-1}, \tag{52}$$

where $\theta_n = \|\lambda_n\|^2$ denotes unknown constant, λ_n is the weight vector of MTN. $\tilde{\theta}_n$ is the estimation error of θ_n with $\tilde{\theta}_n = \theta_n - \hat{\theta}_n$, $\hat{\theta}_n$ is the estimation of θ_n.

In light of (18) and (52), the time derivative of V_n is

$$\dot{V}_n = w_n(u(v) + \sigma_n + \phi_n + k_n \varkappa_n - \dot{x}_{n,c} + \varkappa_{n-1}) + h_n w_n \mathrm{sgn}(\varkappa_n) - \tilde{\theta}_n \dot{\hat{\theta}}_n + \dot{V}_{n-1}. \tag{53}$$

Similar to (21) and (22), by rearranging Lemma 4, we have

$$w_n \phi_n \leq \frac{1}{2} a_n^2 + \frac{1}{2a_n^2} w_n^2 \phi_n^2, \tag{54}$$

$$h_n w_n \mathrm{sgn}(\varkappa_n) \leq \frac{1}{2} h_n^2 + \frac{1}{2} w_n^2, \tag{55}$$

where $a_n > 0$ is a constant.

Substituting (54) and (55) into (53) along with taking (3) and (5) into account, the time derivative of V_n can be rewritten as

$$\begin{aligned}\dot{V}_n &\le w_n(\ell v + \wp(v) + \sigma_n + k_n\varkappa_n - \dot{x}_{n,c} + \varkappa_{n-1}) + \frac{1}{2}a_n^2 + \frac{1}{2a_n^2}w_n^2\phi_n^2 + \frac{1}{2}h_n^2 + \frac{1}{2}w_n^2 - \tilde{\theta}_n\dot{\hat{\theta}}_n + \dot{V}_{n-1}\\ &\le w_n(\ell v + k_n\varkappa_n - w_{n-1}) + w_nF_n + \frac{1}{2}a_n^2 + \frac{1}{2}h_n^2 - w_n^2 + \overline{\wp}w_n - \tilde{\theta}_n\dot{\hat{\theta}}_n + \dot{V}_{n-1},\end{aligned} \tag{56}$$

where $F_n = \sigma_n - \dot{x}_{n,c} + \frac{1}{2a_n^2}w_n\phi_n^2 + \frac{3}{2}w_n + z_{n-1}$ is a combination of nonlinear functions.

Based on the MTN approximation technique in Lemma 5, for any constant $\bar{\varepsilon}_n > 0$, F_n can be approximated by an MTN, that is, the following formula is established

$$F_n = \lambda_n^{\mathrm{T}}P_{m_n}(\boldsymbol{z}_n) + \varepsilon_n(\boldsymbol{z}_n), |\varepsilon_n(\boldsymbol{z}_n)| \le \bar{\varepsilon}_n, \tag{57}$$

where $\boldsymbol{z}_n = [z_1, \ldots, z_n]^{\mathrm{T}}$, $\varepsilon_n(\boldsymbol{z}_n)$ is the approximation error of the combination term F_n and $\lambda_n^{\mathrm{T}}P_{m_n}$.

Furthermore, combining (56) and (57), (58) can be obtained

$$w_nF_n \le w_n\lambda_n^{\mathrm{T}}P_{m_n} + w_n\bar{\varepsilon}_n. \tag{58}$$

Then, according Lemma 4, (58) can be rewritten as

$$w_nF_n \le \frac{1}{2}l_n^2 + \frac{1}{2l_n^2}w_n^2\theta_nP_{m_n}^{\mathrm{T}}P_{m_n} + \frac{1}{2}w_n^2 + \frac{1}{2}\bar{\varepsilon}_n^2, \tag{59}$$

where $l_n > 0$ is the constant.

Substituting (59) into (56) gives

$$\begin{aligned}\dot{V}_n \le{}& \ell w_nv + \overline{\wp}w_n + k_nw_n\varkappa_n - w_{n-1}w_n + \frac{1}{2}l_n^2 + \frac{1}{2l_n^2}w_n^2\theta_nP_{m_n}^{\mathrm{T}}P_{m_n} + \frac{1}{2}\bar{\varepsilon}_n^2\\ &+ \frac{1}{2}a_n^2 + \frac{1}{2}h_n^2 - \frac{1}{2}w_n^2 - \tilde{\theta}_n\dot{\hat{\theta}}_n + \dot{V}_{n-1}.\end{aligned} \tag{60}$$

Define the actual control signal as follows

$$v = \frac{1}{\ell}\mu N(\chi)\left(k_nz_n + \frac{1}{2l_n^2}w_n\hat{\theta}_nP_{m_n}^{\mathrm{T}}P_{m_n} + s_nw_n^{\gamma}\right), \tag{61}$$

where $\mu > 0$ is a positive parameter to adjust the Nussbaum-type function $N(\chi)$. $\ell > 0$, $k_n > 0$, $0 < \gamma \le 1$ and $s_n > 0$ are all design parameters.

Applying Lemma 4 yields that

$$\overline{\wp}w_n \le \frac{1}{2}w_n^2 + \frac{1}{2}\overline{\wp}^2. \tag{62}$$

With the help of the actual control signal v, and taking (51), (60) into account, the time derivative of V_n becomes

$$\begin{aligned}\dot{V}_n &\le \mu N(\chi)\left(k_nz_n + \frac{1}{2l_n^2}w_n\hat{\theta}_nP_{m_n}^{\mathrm{T}}P_{m_n} + s_nw_n^{\gamma}\right)w_n + \frac{1}{2}\overline{\wp}^2 + k_nw_n\varkappa_n\\ &\quad - w_nw_{n-1} + \frac{1}{2}a_n^2 + \frac{1}{2}l_n^2 + \frac{1}{2}\bar{\varepsilon}_n^2 + \frac{1}{2}h_n^2 + \frac{1}{2l_n^2}w_n^2\theta_nP_{m_n}^{\mathrm{T}}P_{m_n} - \tilde{\theta}_n\dot{\hat{\theta}}_n + \dot{V}_{n-1}\\ &\le (\mu N(\chi) + 1)\dot{\chi} - \tau_{11}s_1w_1^{1+\gamma} - \sum_{j=2}^{n}s_jw_j^{1+\gamma} - \tau_{11}k_1w_1^2 - \sum_{j=2}^{n}k_jw_j^2\\ &\quad + \frac{1}{2}\overline{\wp}^2 + \sum_{j=1}^{n}\tilde{\theta}_j\left(\frac{1}{2l_j^2}w_j^2P_{m_j}^{\mathrm{T}}P_{m_j} - \dot{\hat{\theta}}_j\right) + \sum_{j=1}^{n}\left(\frac{1}{2}a_j^2 + \frac{1}{2}h_j^2 + \frac{1}{2}l_j^2 + \frac{1}{2}\bar{\varepsilon}_j^2\right),\end{aligned} \tag{63}$$

where $\dot{\chi} = k_nz_nw_n + \frac{1}{2l_n^2}w_n^2\hat{\theta}_nP_{m_n}^{\mathrm{T}}P_{m_n} + s_nw_n^{1+\gamma}$.

3.2 | Stability analysis of the system

Analyzing the controller design process above, this article takes the following Lyapunov function V into account

$$V = V_n = \frac{1}{2}\sum_{j=1}^{n} w_j^2 + \frac{1}{2}\sum_{j=1}^{n} \tilde{\theta}_j^2. \tag{64}$$

Then, the time derivative of the Lyapunov function is

$$\begin{aligned}\dot{V} \le{}& (\mu N(\chi)+1)\dot{\chi} - \tau_{11}s_1 w_1^{1+\gamma} - \sum_{j=2}^{n} s_j w_j^{1+\gamma} - \tau_{11}k_1 w_1^2 - \sum_{j=2}^{n} k_j w_j^2 \\ &+ \sum_{j=1}^{n}\tilde{\theta}_j\left(\frac{1}{2l_j^2}w_j^2 P_{m_j}^{\mathrm{T}} P_{m_j} - \dot{\hat{\theta}}_j\right) + \sum_{j=1}^{n}\left(\frac{1}{2}a_j^2 + \frac{1}{2}h_j^2 + \frac{1}{2}l_j^2 + \frac{1}{2}\bar{\varepsilon}_j^2\right) + \frac{1}{2}\bar{\wp}^2.\end{aligned} \tag{65}$$

According to (65), the adaptive law can be designed as

$$\dot{\hat{\theta}}_j = \frac{1}{2l_j^2}w_j^2 P_{m_j}^{\mathrm{T}} P_{m_j} - \sigma\hat{\theta}_j, \tag{66}$$

where $\sigma > 0$ is the design parameter.

Substituting (66) into (65) yields that

$$\dot{V} \le (\mu N(\chi)+1)\dot{\chi} - \tau_{11}s_1 w_1^{1+\gamma} - \sum_{j=2}^{n} s_j w_j^{1+\gamma} - \tau_{11}k_1 w_1^2 - \sum_{j=2}^{n} k_j w_j^2 + \sigma\hat{\theta}\tilde{\theta} + \frac{1}{2}\bar{\wp}^2 + \sum_{j=1}^{n}\left(\frac{1}{2}a_j^2 + \frac{1}{2}h_j^2 + \frac{1}{2}l_j^2 + \frac{1}{2}\bar{\varepsilon}_j^2\right). \tag{67}$$

Applying Lemma 4 to deal with $\sigma\hat{\theta}\tilde{\theta}$, one has

$$\sigma\hat{\theta}\tilde{\theta} \le -\frac{1}{2}\sigma\tilde{\theta}^2 + \frac{1}{2}\sigma\theta^2. \tag{68}$$

Substituting (68) into (67), the time derivative of the Lyapunov function V is

$$\begin{aligned}\dot{V} \le{}& -\tau_{11}s_1 w_1^{1+\gamma} - \sum_{j=2}^{n} s_j w_j^{1+\gamma} - \tau_{11}k_1 w_1^2 - \sum_{j=2}^{n} k_j w_j^2 - \frac{1}{2}\sigma\tilde{\theta}^2 - \sigma\left(\frac{1}{2}\tilde{\theta}^2\right)^{\frac{1+\gamma}{2}} + \sigma\left(\frac{1}{2}\tilde{\theta}^2\right)^{\frac{1+\gamma}{2}} \\ &+ \frac{1}{2}\sigma\theta^2 + \frac{1}{2}\bar{\wp}^2 + \sum_{j=1}^{n}\left(\frac{1}{2}a_j^2 + \frac{1}{2}h_j^2 + \frac{1}{2}l_j^2 + \frac{1}{2}\bar{\varepsilon}_j^2\right) + (\mu N(\chi)+1)\dot{\chi}.\end{aligned} \tag{69}$$

By utilizing Lemma 3 to deal with $\sigma\left(\frac{1}{2}\tilde{\theta}^2\right)^{\frac{1+\gamma}{2}}$, there exists a constant $\nu(0<\nu<1)$ such that

$$\sigma\left(\frac{1}{2}\tilde{\theta}^2\right)^{\frac{1+\gamma}{2}} \le \sigma\nu\frac{1}{2}\tilde{\theta}^2 + \sigma\frac{1-\gamma}{2}\left(\frac{(1+\gamma)}{2\nu}\right)^{\frac{1+\gamma}{1-\gamma}}. \tag{70}$$

Substituting (70) into (69) and taking Lemma 6 into account yields

$$\begin{aligned}\dot{V} \le{}& -\tau_{11}k_1 w_1^2 - \sum_{j=2}^{n} k_j w_j^2 - \tau_{11}s_1 w_1^{1+\gamma} - \sum_{j=2}^{n} s_j w_j^{1+\gamma} - \frac{1}{2}(1-\nu)\sigma\tilde{\theta}^2 - \sigma\left(\frac{1}{2}\tilde{\theta}^2\right)^{\frac{1+\gamma}{2}} \\ &+ \sigma\frac{1-\gamma}{2}\left(\frac{(1+\gamma)}{2\nu}\right)^{\frac{1+\gamma}{1-\gamma}} + \frac{1}{2}\sigma\theta^2 + \frac{1}{2}\bar{\wp}^2 + \sum_{j=1}^{n}\left(\frac{1}{2}a_j^2 + \frac{1}{2}h_j^2 + \frac{1}{2}l_j^2 + \frac{1}{2}\bar{\varepsilon}_j^2\right) + (\mu N(\chi)+1)\dot{\chi}\end{aligned}$$

$$
\begin{aligned}
&= -\sum_{j=2}^{n} m_j w_j^2 - \sum_{j=2}^{n} q_j w_j^{1+\gamma} - \frac{1}{2}(1-\nu)\sigma\tilde{\theta}^2 - \sigma\left(\frac{1}{2}\tilde{\theta}^2\right)^{\frac{1+\gamma}{2}} + \sigma\frac{1-\gamma}{2}\left(\frac{\nu^{-1}(1+\gamma)}{2}\right)^{\frac{1+\gamma}{1-\gamma}} + \frac{1}{2}\sigma\theta^2 \\
&\quad + \frac{1}{2}\overline{\wp}^2 + \sum_{j=1}^{n}\left(\frac{1}{2}a_j^2 + \frac{1}{2}h_j^2 + \frac{1}{2}l_j^2 + \frac{1}{2}\bar{\varepsilon}_j^2\right) + (\mu N(\chi)+1)\dot{\chi} \\
&\le -\eta_1 V - \eta_2 V^{\frac{1+\gamma}{2}} + \bar{\imath} + (\mu N(\chi)+1)\dot{\chi},
\end{aligned} \tag{71}
$$

where $m_1 = \tau_{11}k_1$, $m_j = k_j$, $q_1 = \tau_{11}s_1$, $q_i = s_j, j = 2, \ldots, n$, $\eta_1 = \min\{2m_j, (1-\nu)\sigma\} > 0$, $\eta_2 = \min\{2q_j, \sigma\} > 0$, $\bar{\imath} = \frac{1}{2}\sigma\theta^2 + \frac{1}{2}\overline{\wp}^2 + \sigma\frac{1-\gamma}{2}\left(\frac{(1+\gamma)}{2\nu}\right)^{\frac{1+\gamma}{1-\gamma}} + \sum_{j=1}^{n}\left(\frac{1}{2}a_j^2 + \frac{1}{2}h_j^2 + \frac{1}{2}l_j^2 + \frac{1}{2}\bar{\varepsilon}_j^2\right)$.

Based on the proof process in Reference 57 and Lemma 1, it can be obtained that $(\mu N(\chi)+1)\dot{\chi}$ is bounded on $[0, t_q)$. As a result, there exists a constant $\tilde{\imath} > 0$ such that $\max_{t\in[0,t_q)} |(\mu N(\chi)+1)\dot{\chi}| \le \tilde{\imath}$ hold. Let $\imath = \bar{\imath} + \tilde{\imath}$, (71) can be recomputed as

$$
\dot{V} \le -\eta_1 V - \eta_2 V^{\frac{1+\gamma}{2}} + \imath. \tag{72}
$$

Furthermore, (72) is equivalent to the following two inequalities

$$
\begin{aligned}
\dot{V} &\le -\kappa\eta_1 V + \kappa\eta_1 V - \eta_1 V - \eta_2 V^{\frac{1+\gamma}{2}} + \imath \\
&= -\kappa\eta_1 V - (1-\kappa)\eta_1 V - \eta_2 V^{\frac{1+\gamma}{2}} + \imath
\end{aligned} \tag{73}
$$

or

$$
\begin{aligned}
\dot{V} &\le -\eta_1 V - \eta_2 V^{\frac{1+\gamma}{2}} + \kappa\eta_2 V^{\frac{1+\gamma}{2}} - \kappa\eta_2 V^{\frac{1+\gamma}{2}} + \imath \\
&= -\eta_1 V - (1-\kappa)\eta_2 V^{\frac{1+\gamma}{2}} - \kappa\eta_2 V^{\frac{1+\gamma}{2}} + \imath,
\end{aligned} \tag{74}
$$

where $0 < \kappa < 1$ is a constant.

Then, according to (73), if $V > \frac{\imath}{(1-\kappa)\eta_1}$ holds, one has

$$
\dot{V} \le -\kappa\eta_1 V - \eta_2 V^{\frac{1+\gamma}{2}}. \tag{75}
$$

Thus, by applying Lemma 2, it is obvious that w_k, $\varkappa_n$, $\tilde{\theta}$ will converge into the following region

$$
(w_k, \varkappa_n, \tilde{\theta}) \in \left\{ V \le \frac{\imath}{(1-\kappa)\eta_1} \right\} \tag{76}
$$

in the finite time $T_1\left(T_1 \le \frac{2}{\kappa\eta_1(1-\gamma)} \ln \frac{\kappa\eta_1 V^{\frac{1-\gamma}{2}}(0) + \eta_2}{\eta_2}\right)$.

Similarly, according to (74), if $V^{\frac{1+\gamma}{2}} > \frac{\imath}{(1-\kappa)\eta_2}$ holds, one has

$$
\dot{V} \le -\eta_1 V - \kappa\eta_2 V^{\frac{1+\gamma}{2}}. \tag{77}
$$

Then, by applying Lemma 2, it is obvious that w_k, $\varkappa_n$, $\tilde{\theta}$ will converge into the following region

$$
(w_k, \varkappa_n, \tilde{\theta}) \in \left\{ V \le \left(\frac{\imath}{(1-\kappa)\eta_2}\right)^{\frac{2}{1+\gamma}} \right\} \tag{78}
$$

in the finite time $T_2\left(T_2 \le \frac{2}{\eta_1(1-\gamma)} \ln \frac{\eta_1 V^{\frac{1-\gamma}{2}}(0) + \kappa\eta_2}{\kappa\eta_2}\right)$.

Therefore, $\varkappa_n$, $\tilde{\theta}$ achieve SGUUB in a finite time $T(T = \max\{T_1, T_2\})$ can be guaranteed.

Then, based on (75) and (78), it follows that $\varkappa_1$ and w_1 can converge into the following region in a finite time T

$$|w_1| \leq \min\left\{\sqrt{\frac{2\iota}{(1-\kappa)\eta_1}}, \sqrt{2\left(\frac{\iota}{(1-\kappa)\eta_2}\right)^{\frac{2}{1+\gamma}}}\right\}, \tag{79}$$

$$|\varkappa_1| \leq \min\left\{\sqrt{\frac{2\iota}{(1-\kappa)\eta_1}}, \sqrt{2\left(\frac{\iota}{(1-\kappa)\eta_2}\right)^{\frac{2}{1+\gamma}}}\right\}. \tag{80}$$

Thus, for $\forall t \geq T$, z_1 satisfies

$$|z_1| \leq |\varkappa_1| + |w_1| \leq \min\left\{2\sqrt{\frac{2\iota}{(1-\kappa)\eta_1}}, 2\sqrt{2\left(\frac{\iota}{(1-\kappa)\eta_2}\right)^{\frac{2}{1+\gamma}}}\right\}. \tag{81}$$

This shows that by selecting the right parameters, the tracking error z_1 can be infinitely small in finite-time. Finally, according to the above analysis, it is obvious that all signals including p, I, w_j, $\varkappa_j$, $\hat{\dot{\theta}}_j$, $\tilde{\theta}_j$, z_j, v in the close-loop system are SGUUB in the finite-time T.

Remark 7. By analyzing the expressions for η_1, η_2 and ι, we can conclude that larger k_j, s_j and smaller h_j can make sure the tracking error z_1 is arbitrarily small.

Eventually, according to the above analysis, the main results of this article can be summarized as the following theorem.

Theorem 1. *Consider the nonlinear system (1) subject to backlash-like input hysteresis and multiple objective constraints satisfying Assumption 1. If the actual controller is designed as (61), and the virtual control signal is described as (27), (39), (50) with the adaptive law given as (66), the controller can be designed to ensure*

(1) All signals in the closed-loop system can be guaranteed finite-time SGUUB.
(2) The tracking error is regulated to a sufficiently small neighborhood of the original point within a finite time.
(3) Multiple objective constraints can be realized.

Remark 8. Figure 2 displays the diagram of the proposed control process.

4 | SIMULATION RESULTS

In this section, a simulation example is given to prove the validity of the adaptive finite-time controller proposed in Theorem 1.

Example: To verify the effectiveness of the adaptive finite-time control method proposed in this article, a class of longitudinal model of uncertain aircraft is considered. According to the work of Reference 58, its dynamics model can be described as follows

$$\begin{cases} \dot{x}_1 = g_1 x_2 + \sigma_1(\bar{\boldsymbol{x}}_1) + \phi_1(\bar{\boldsymbol{x}}_1, t), \\ \dot{x}_2 = g_2 x_3 + \sigma_2(\bar{\boldsymbol{x}}_2) + \phi_2(\bar{\boldsymbol{x}}_2, t), \\ \dot{x}_3 = g_3 u(v) + \sigma_2(\bar{\boldsymbol{x}}_3) + \phi_2(\bar{\boldsymbol{x}}_3, t), \\ y = x_1, \end{cases} \tag{82}$$

where $\sigma_1(\bar{\boldsymbol{x}}_1) = -\frac{g}{V_T}\cos x_1 + \overline{L}_0$, $\sigma_2(\bar{\boldsymbol{x}}_2) = \frac{g}{V_T}\cos x_1 - \overline{L}_0 - \overline{L}_\partial x_2$, $\sigma_3(\bar{\boldsymbol{x}}_3) = Q_\partial x_2 + Q_\Im x_3$, $g_1 = \overline{L}_\partial > 0$, $g_2 = \overline{L}_\hbar > 0$, $g_3 = Q_\delta > 0$. The unknown physical parameters are $\overline{L}_0 = -0.1$, $\overline{L}_\partial = 1$, $\overline{L}_\hbar = 1$, $Q_\partial = 0.1$, $Q_\Im = -0.02$, acceleration of gravity is

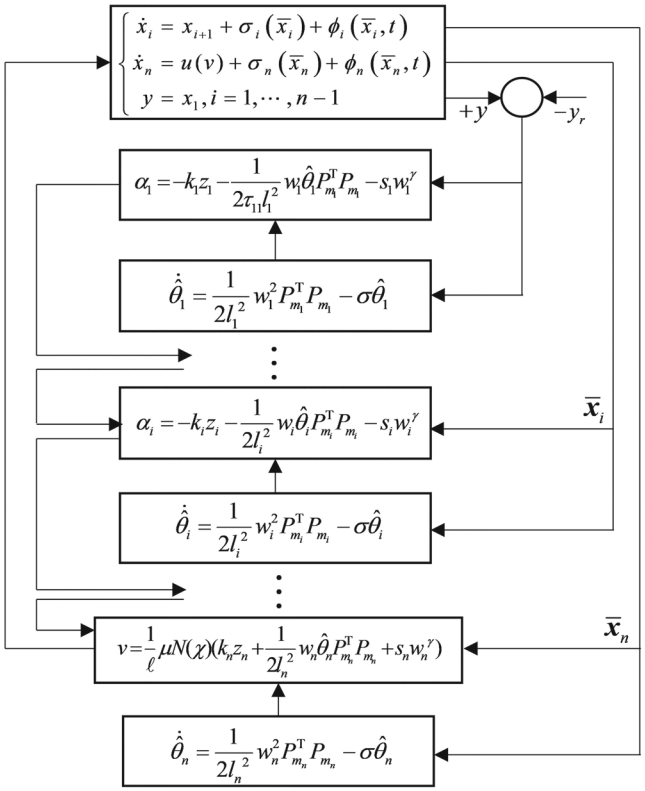

FIGURE 2 The diagram of the proposed control process.

TABLE 1 Design parameter.

Parameter	Value
The initial state of the controlled system	$\boldsymbol{x}(\mathbf{0}) = [x_1(0), x_2(0), x_3(0)]^{\mathrm{T}} = [0, 0, 0]^{\mathrm{T}}$
Reference signal	$y_r = 0.45 \sin t$
Controller parameters	$k_1 = 8, k_2 = 20, k_3 = 50, l_j = 1, s_j = 0.1, \ell = 3, \mu = 0.3$
Adaptive law parameters	$l_j = 1, \sigma = 1$
Error compensation system parameters	$k_1 = 8, k_2 = 20, k_3 = 50, h_1 = 0.01, h_2 = h_3 = 0.05$
Backlash-like hysteresis parameters	$\overline{\psi} = 1, \ell = 3, \mathfrak{T} = 0.4$

$g = 9.8m/s^2$, $V_T = 200m/s$ denotes steady speed. $\phi_1(\bar{\boldsymbol{x}}_1, t) = 0.01 \sin 2t$, $\phi_2(\bar{\boldsymbol{x}}_2, t) = 0.1 \cos 2t$, $\phi_3(\bar{\boldsymbol{x}}_3, t) = 0.05 \sin t \cos 2t$. $b_{\varsigma_1}(t) = 0.7 + 0.1 \sin t$ and $b_{\varsigma_2}(t) = 0.9 + 0.1 \sin t$ are constraints functions. Three objective functions are defined on $I \in \Omega := \{I \in R : -b_{\varsigma_1}(t) < I < b_{\varsigma_2}(t)\}$, whose expression are described as follows

case 1: $I_1 = x_1$;
case 2: $I_2 = x_1 + 0.01x_1^2$
case 3: $I_3 = x_1 + 0.05x_1^2 + 0.05x_1^3$.

The required parameters during the design of the controller are shown in the following Table 1.

According to Theorem 1, two virtual control signals, the actual controller and the adaptive law are designed as follows

$$\alpha_1 = -k_1 z_1 - \frac{1}{2\tau_{11} l_1^2} w_1 \hat{\theta}_1 P_{m_1}^{\mathrm{T}} P_{m_1} - s_1 w_1^{\gamma}, \tag{83}$$

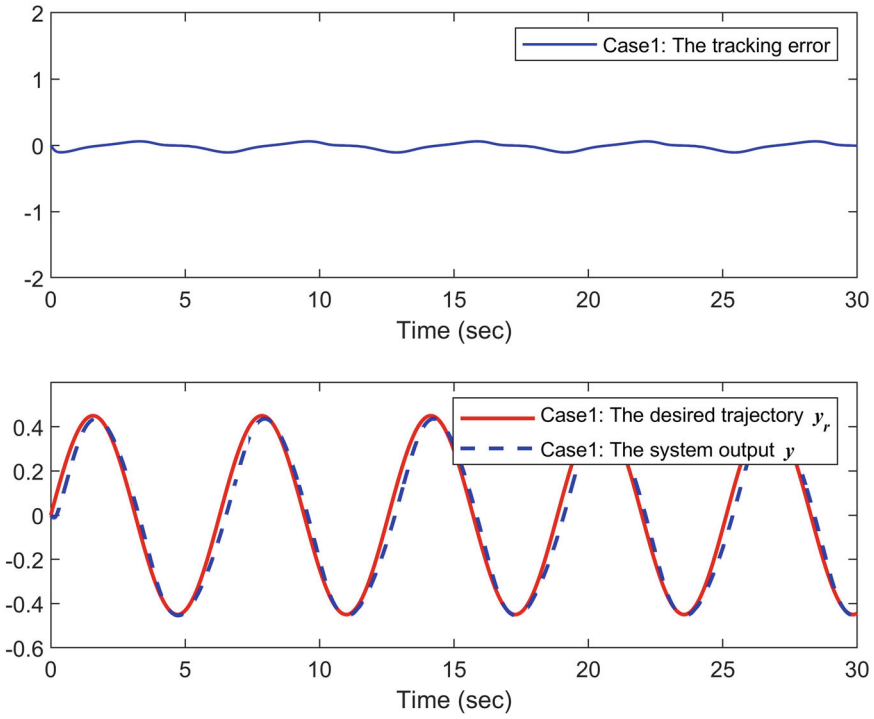

FIGURE 3 The tracking error trajectory and tracking effect in case1.

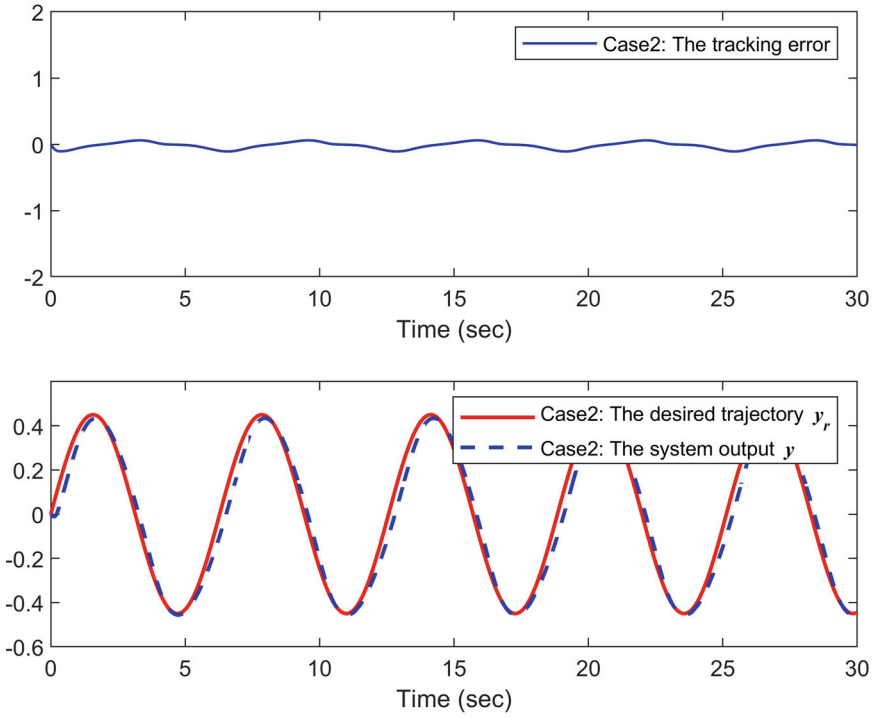

FIGURE 4 The tracking error trajectory and tracking effect in case 2.

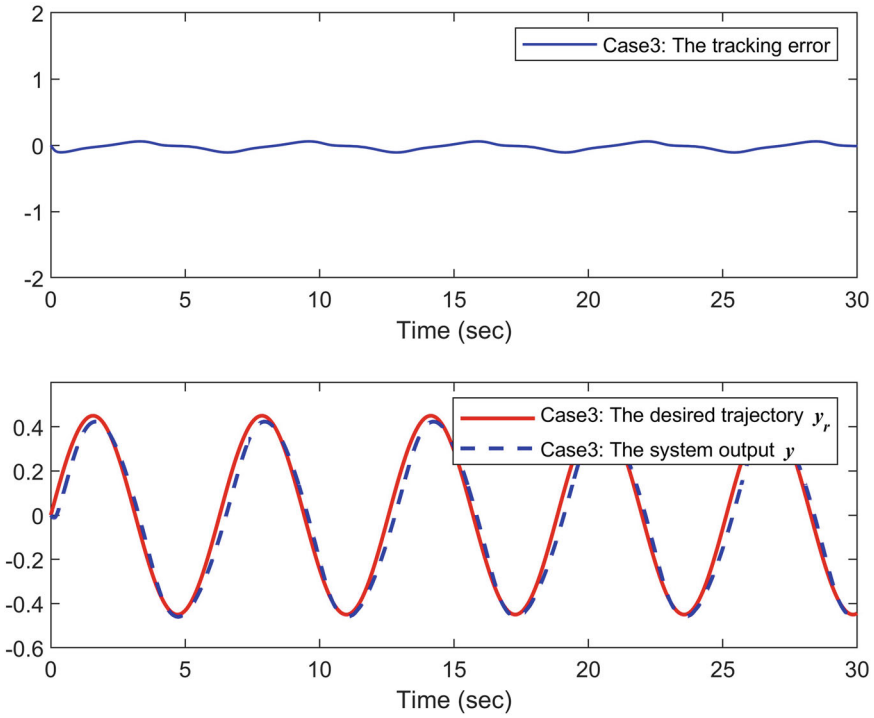

FIGURE 5 The tracking error trajectory and tracking effect in case 3.

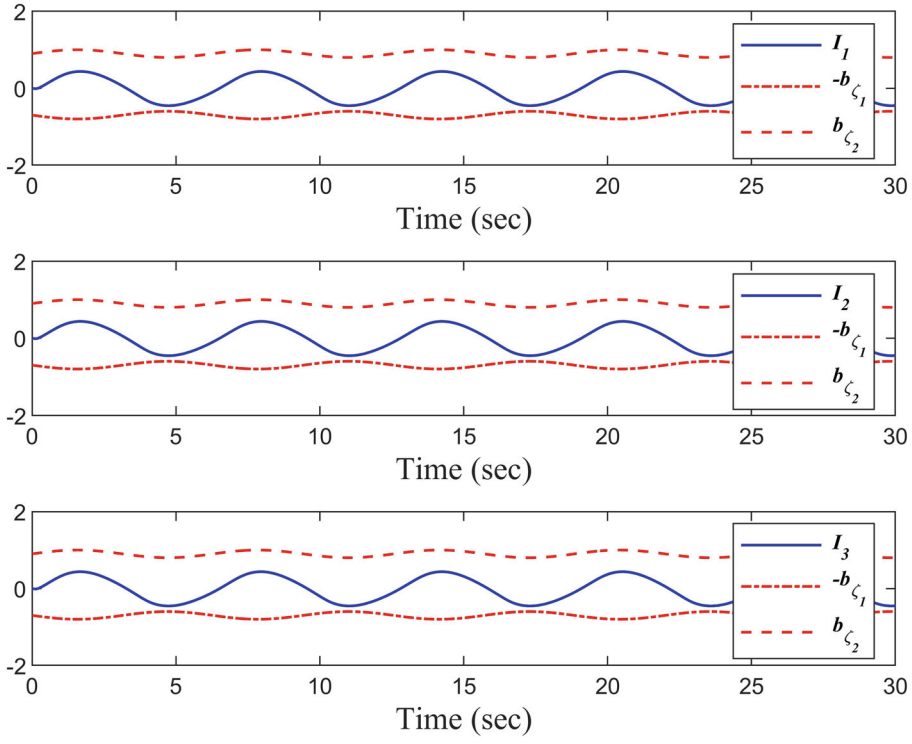

FIGURE 6 Trajectories of multiple objective functions and constraint functions.

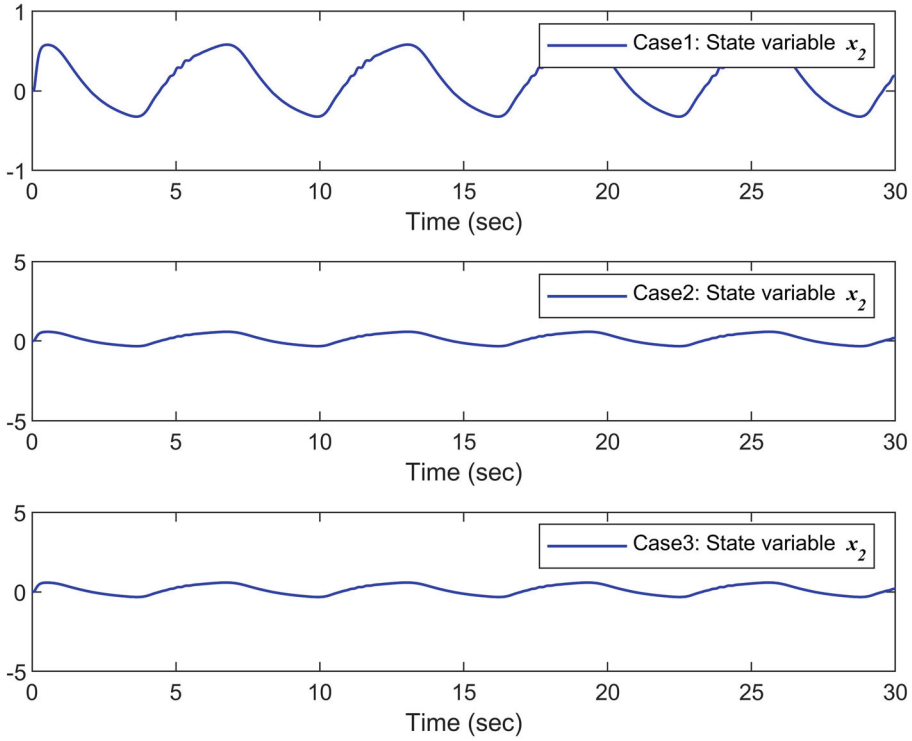

FIGURE 7 State variables x_2.

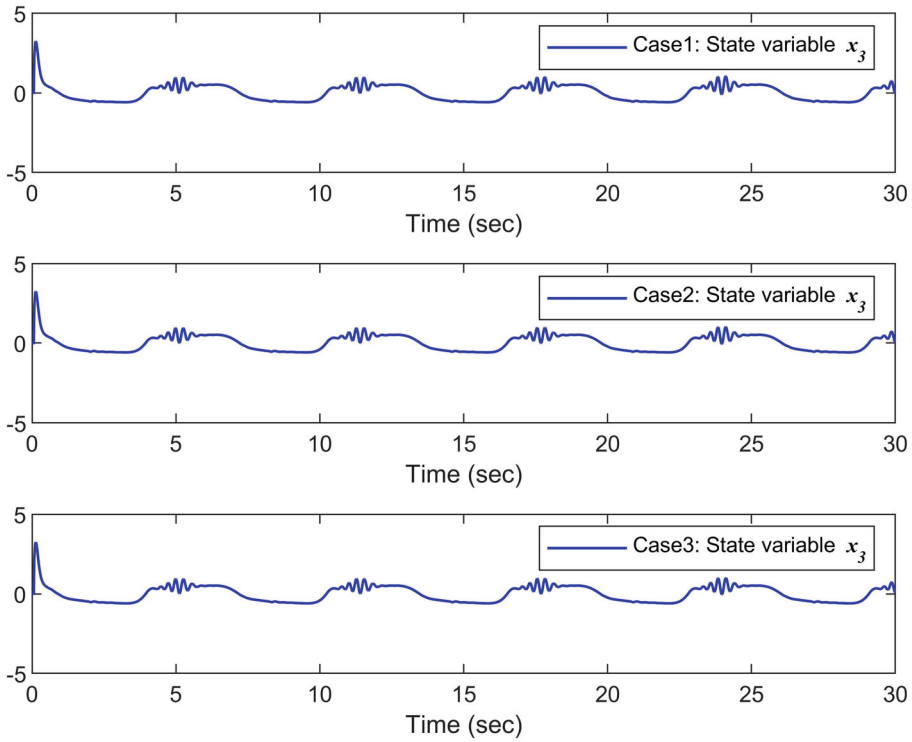

FIGURE 8 State variables x_3.

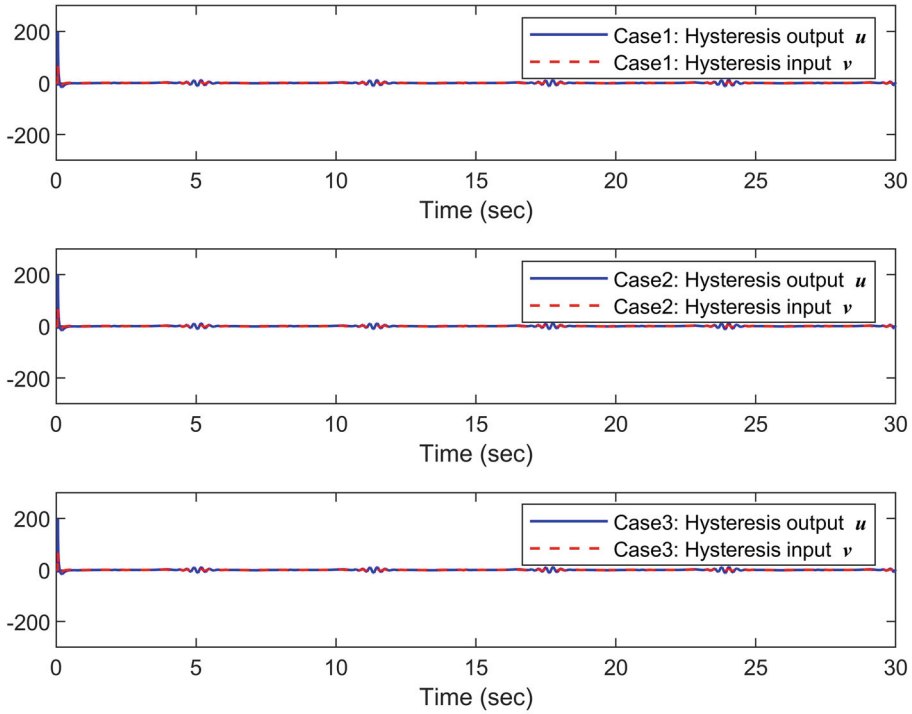

FIGURE 9 Hysteresis output and input in three cases.

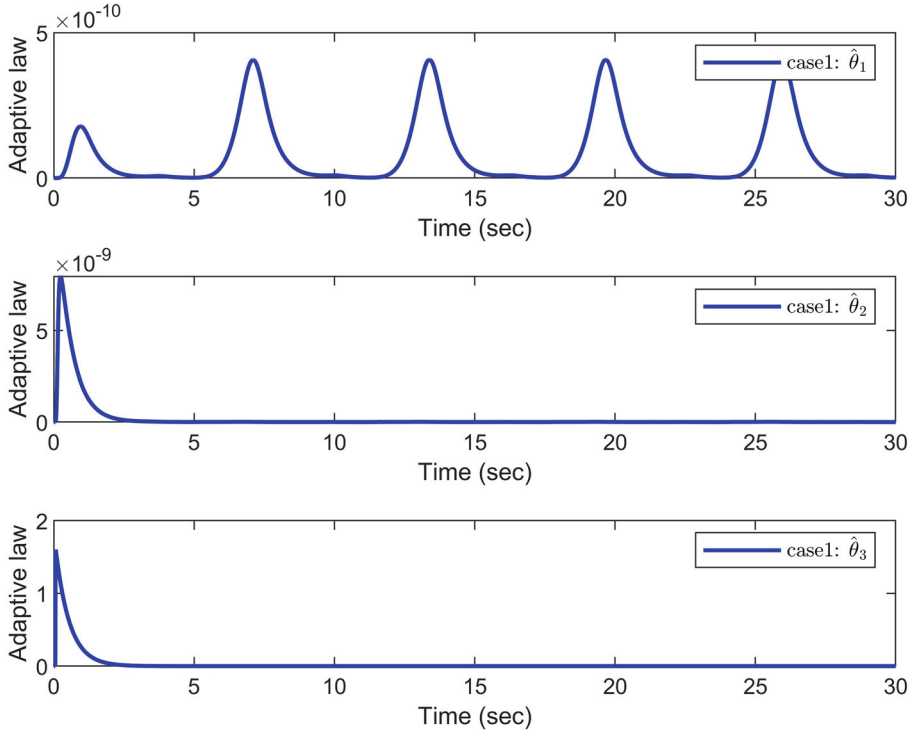

FIGURE 10 The responses of $\|\lambda_j\|^2$ in case 1.

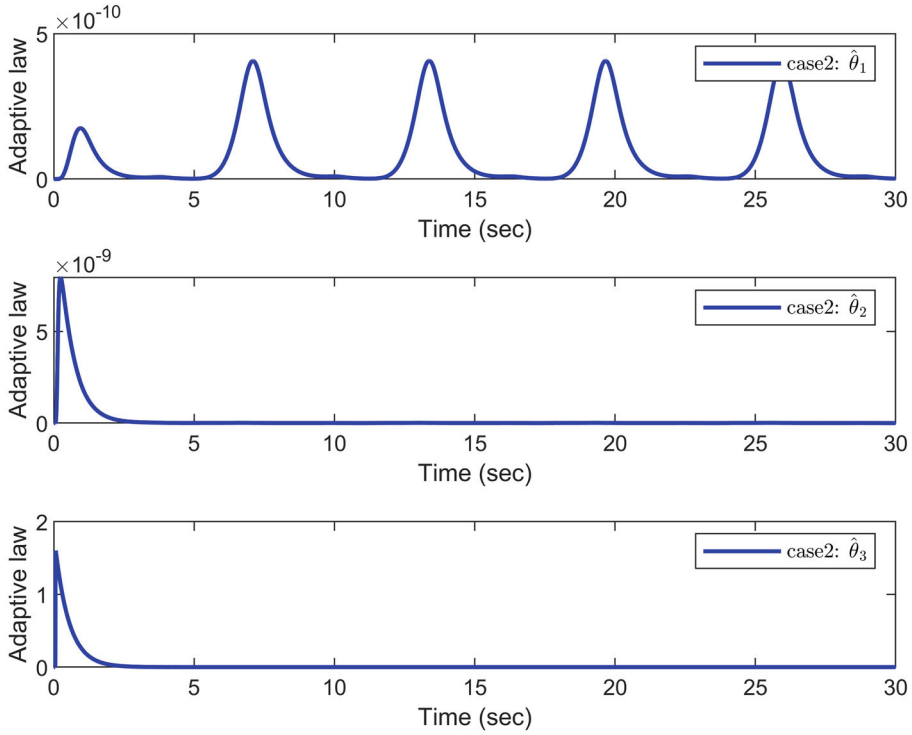

FIGURE 11 The responses of $\|\lambda_j\|^2$ in case 2.

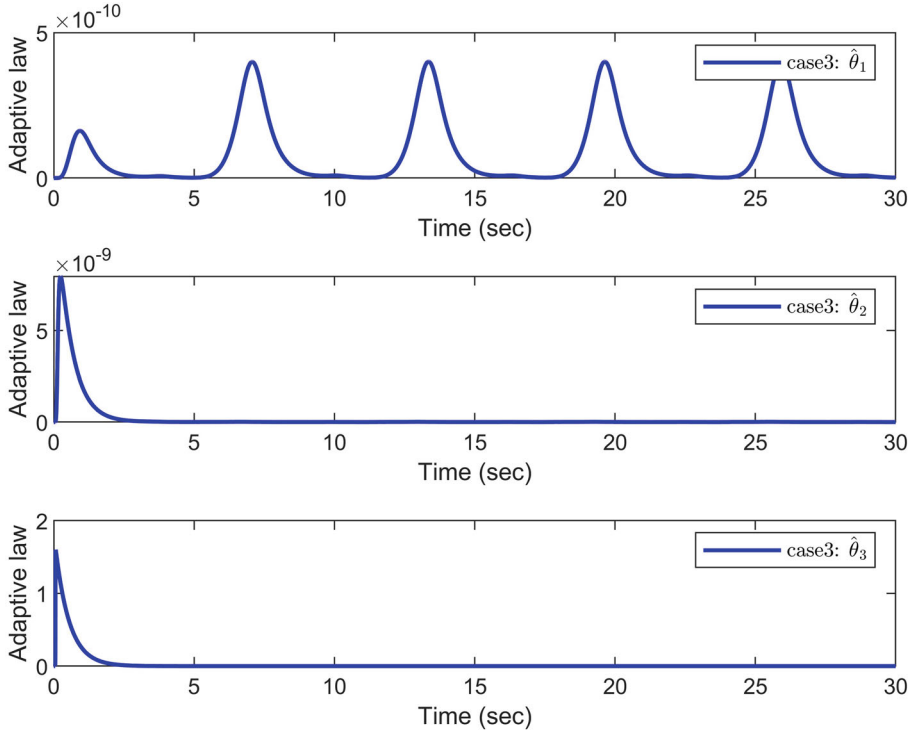

FIGURE 12 The responses of $\|\lambda_j\|^2$ in case 3.

$$\alpha_2 = -k_2 z_2 - \frac{1}{2l_2^2} w_2 \hat{\theta}_2 P_{m_2}^{\mathrm{T}} P_{m_2} - s_2 w_2^{\gamma}, \tag{84}$$

$$v = \frac{1}{\ell} \mu N(\chi) \left(k_3 z_3 + \frac{1}{2l_3^2} w_3 \hat{\theta}_3 P_{m_3}^{\mathrm{T}} P_{m_3} + s_3 w_3^{\gamma} \right), \tag{85}$$

$$\dot{\hat{\theta}}_j = \frac{1}{2l_j^2} w_j^2 P_{m_j}^{\mathrm{T}} P_{m_j} - \sigma \hat{\theta}_j, \quad j = 1, 2, 3, \tag{86}$$

where $N(\chi) = \chi^2 \cos \chi$, $\dot{\chi} = k_3 z_3 w_3 + \frac{1}{2l_3^2} w_3^2 \hat{\theta}_3 P_{m_3}^{\mathrm{T}} P_{m_3} + s_3 w_3^{1+\gamma}$, $\gamma = 0.6$, $z_1 = x_1 - y_r$, $z_2 = x_2 - \alpha_1$, $z_3 = x_3 - \alpha_2$.

The simulation results are shown in Figures 3–12. Figures 3–5 respectively show the tracking error trajectory and tracking effect in three cases, which show that satisfactory control results can be achieved in three case. Figure 6 shows the trajectories of multiple objective functions and the constraint functions in three cases. Figures 7 and 8 show the state variables x_2 and x_3 in three cases, respectively. Figure 9 shows the hysteresis output and input in three cases. Figures 10–12 shows the adaptive laws $\hat{\theta}_1$, $\hat{\theta}_2$ and $\hat{\theta}_3$ in three cases. The above simulation results show that the control method proposed in this article is effective.

5 | CONCLUSION

This article proposes an adaptive MTN finite-time control scheme based on DSC technique for nonlinear systems with backlash-like hysteresis and multiple objective constraints. In order to confine all the objective constraint functions within their constraint boundaries, a new TVBF is introduced. Then, by combining backstepping method with DSC technique, the problem of "complexity explosion" is avoided. Additionally, an ECS is utilized to reduce the influence of filter error of the command filter on control performance. Moreover, in view of the impact of hysteresis on the stability of the system, the backlash-like hysteresis model is used to approximate the hysteresis nonlinearity which is transformed into a continuous linear combination to avoid "singularity" problem. Accordingly, a novel command filter-based adaptive MTN finite-time control scheme by combining Nussbaum-type function with backstepping method is designed. Finally, a practical simulation is conducted to demonstrate the effectiveness of the proposed scheme. Future research directions may involve extending the investigation toward achieving asymptotic tracking control within a finite-time for nonlinear systems with unknown hysteresis.

FUNDING INFORMATION

This research was supported by the Youth Tutor Visiting Study and Training Project of Shandong Province.

CONFLICT OF INTEREST STATEMENT

The authors declare that they have no conflict of interest.

DATA AVAILABILITY STATEMENT

Data sharing not applicable to this article as no datasets were generated or analyzed during the current study.

ORCID

Wei Zhao https://orcid.org/0009-0002-3316-1911
Yu-Qun Han https://orcid.org/0000-0001-9847-9627

REFERENCES

1. You XX, Dian SY, Liu K, Guo B, Xiang GF, Zhu YQ. Command filter-based adaptive fuzzy finite-time tracking control for uncertain fractional-order nonlinear systems. *IEEE Trans Fuzzy Syst*. 2023;31(1):226-240.
2. Wu J, He FR, Shen H, Ding SH, Wu ZG. Adaptive NN fixed-time fault-tolerant control for uncertain stochastic system with deferred output constraint via self-triggered mechanism. *IEEE Trans Fuzzy Cybern*. 2023;53(9):5892-5903.
3. Guo ZY, Oliveira TR, Guo JG, Wang Z. Performance-guaranteed adaptive asymptotic tracking for nonlinear systems with unknown sign-switching control direction. *IEEE Trans Autom Control*. 2023;68(2):1077-1084.
4. Kang Y, Xi HS, Zhang DL, Ji HB. A robust adaptive control design for a class of uncertain nonlinear Markovian jump systems. *Asian J Control*. 2007;9(1):73-79.

5. Zong GD, Yang D, Lam J, Song XQ. Fault-tolerant control of switched LPV systems: a bumpless transfer approach. *IEEE/ASME Trans Mechatron*. 2022;27(3):1436-1446.
6. Zhan YL, Tong SC. Adaptive fuzzy output-feedback decentralized control for fractional-order nonlinear large-scale systems. *IEEE Trans Cybern*. 2022;52(12):12795-12804.
7. Wang HQ, Kang SJ, Zhao XD, Xu N, Li TS. Command filter-based adaptive neural control design for nonstrict-feedback nonlinear systems with multiple actuator constraints. *IEEE Trans Cybern*. 2022;52(11):12561-12570.
8. Wu J, Chen XM, Zhao QJ, Li J, Wu ZG. Adaptive neural dynamic surface control with prespecified tracking accuracy of uncertain stochastic nonstrict-feedback systems. *IEEE Trans Cybern*. 2022;52(5):3408-3421.
9. He WJ, Zhu SL, Li N, Han YQ. Adaptive controller design for switched stochastic nonlinear systems subject to unknown dead-zone input via new type of network approach. *Int J Control Autom Syst*. 2023;21(2):499-507.
10. Wang N, Tao FZ, Fu ZM, Song SZ. Adaptive fuzzy control for a class of stochastic strict feedback high-order nonlinear systems with full-state constraints. *IEEE Trans Syst Man Cybern Syst*. 2022;52(1):205-213.
11. Wu J, Wang W, Ding SH, Xie XP, Yi Y. Adaptive neural optimized control for uncertain strict-feedback systems with unknown control directions and pre-set performance. *Commun Nonlinear Sci Numer Simul*. 2023;126:107506.
12. Zhan YL, Sui S, Tong SC. Adaptive fuzzy decentralized dynamic surface control for fractional-order nonlinear large-scale systems. *IEEE Trans Fuzzy Syst*. 2022;30(8):3373-3383.
13. Wang HQ, Xu K, Liu PXP, Qiao JF. Adaptive fuzzy fast finite-time dynamic surface tracking control for nonlinear systems. *IEEE Trans Circuits Syst I Regular Pap*. 2021;68(10):4337-4348.
14. Li YM, Li YX, Tong SC. Event-based finite-time control for nonlinear multiagent systems with asymptotic tracking. *IEEE Trans Autom Control*. 2023;68(6):3790-3797.
15. Wang N, Fu ZM, Tao FZ, Song SZ, Wang T. A simplified adaptive tracking control for nonlinear pure-feedback systems with input delay and full-state constraints. *Int J Adapt Control Signal Process*. 2021;35(12):2521-2536.
16. Liu L, Li XS, Liu YJ, Tong SC. Neural network based adaptive event trigger control for a class of electromagnetic suspension systems. *Control Eng Pract*. 2021;106:104675.
17. Han YQ, He WJ, Li N, Zhu SL. Adaptive tracking control of a class of nonlinear systems with input delay and dynamic uncertainties using multi-dimensional Taylor network. *Int J Control Autom Syst*. 2021;19(12):4078-4089.
18. Li N, Zhu SL, He WJ, Han YQ. Controller design for nonlinear systems subject to both input saturation and asymmetry time-varying state constraints: a novel network-based approach. *Int J Adapt Control Signal Process*. 2022;36(12):3124-3141.
19. He WJ, Zhu SL, Li N, Han YQ. Novel adaptive controller design for a class of switched nonlinear systems subject to input delay using multi-dimensional Taylor network. *Int J Adapt Control Signal Process*. 2021;36(3):607-624.
20. Tong SC, Li YM, Feng G, Li TS. Observer-based adaptive fuzzy backstepping dynamic surface control for a class of MIMO nonlinear systems. *IEEE Trans Syst Man Cybern*. 2011;41(4):1124-1135.
21. Liu X, Tong DB, Chen QY, Zhou WN, Shen SG. Observer-based adaptive funnel dynamic surface control for nonlinear systems with unknown control coefficients and hysteresis input. *Neural Process Lett*. 2022;54(6):4681-4710.
22. Ma JJ, Zheng ZQ, Li P. Adaptive dynamic surface control of a class of nonlinear systems with unknown direction control gains and input saturation. *IEEE Trans Cybern*. 2015;45(4):728-741.
23. Xu YM, Liu JP, Yu JP, Wang QG. Adaptive neural networks command filtered control for MIMO nonlinear discrete-time systems with input constraint. *IEEE Trans Circuits Syst*. 2023;70(2):581-585.
24. Li YX. Command filter adaptive asymptotic tracking of uncertain nonlinear systems with time-varying parameters and disturbances. *IEEE Trans Autom Control*. 2022;67(6):2973-2980.
25. Huang LT, Li YM, Tong SC. Command filter-based adaptive fuzzy backstepping control for a class of switched non-linear systems with input quantisation. *IET Control Theory Appl*. 2017;11(12):1948-1958.
26. Zhang J, Li S, Ahn CK, Xiang ZR. Decentralized event-triggered adaptive fuzzy control for nonlinear switched large-scale systems with input delay via command-filtered backstepping. *IEEE Trans Fuzzy Syst*. 2022;30(6):2118-2123.
27. Ma LD, Wang X, Zhou YH. Observer and command-filter-based adaptive neural network control algorithms for nonlinear multi-agent systems with input delay. *Cogn Comput*. 2022;14(2):814-827.
28. Li KW, Li YM. Adaptive fuzzy finite-time dynamic surface control for high-order nonlinear system with output constraints. *Int J Control Autom Syst*. 2021;19(1):112-123.
29. Li KW, Li YM. Adaptive neural network finite-time dynamic surface control for nonlinear systems. *IEEE Trans Neural Networks Learn Syst*. 2021;32(12):5688-5697.
30. Wang HQ, Kang SJ, Feng ZG. Finite-time adaptive fuzzy command filtered backstepping control for a class of nonlinear systems. *Int J Fuzzy Syst*. 2019;21(8):2575-2587.
31. Li N, Han YQ, He WJ, Zhu SL. Control design for stochastic nonlinear systems with full-state constraints and input delay: a new adaptive approximation method. *Int J Control Autom Syst*. 2022;20(8):2768-2778.
32. Gao TT, Li TS, Liu YJ, Tong SC. IBLF-based adaptive neural control of state-constrained uncertain stochastic nonlinear systems. *IEEE Trans Neural Networks Learn Syst*. 2022;33(12):7345-7356.
33. Liu L, Gao TT, Liu YJ, Tong SC, Chen CLP, Ma L. Time-varying IBLFs-based adaptive control of uncertain nonlinear systems with full state constraints. *Automatica*. 2021;129:109595.
34. Wang K, Liu XP, Jing YW. Adaptive finite-time command filtered controller design for nonlinear systems with output constraints and input nonlinearities. *IEEE Trans Neural Networks Learn Syst*. 2022;33(11):6893-6904.

35. Ma YK, Ji HB, Liu W. Adaptive stabilization for a class of stochastic nonlinear systems with Prandtl-Ishlinskii hysteresis. *Asian J Control*. 2014;16(2):539-545.
36. Xu N, Chen Y, Xue AK, Zong GD, Zhao XD. Adaptive tracking control of time-varying delay switched nonstrict-feedback nonlinear systems with unknown backlash-like hysteresis. *Int J Adapt Control Signal Process*. 2022;36(7):1584-1602.
37. Lv WS, Wang F. Finite-time adaptive fuzzy tracking control for a class of nonlinear systems with unknown hysteresis. *Int J Fuzzy Syst*. 2018;20(3):782-790.
38. He WJ, Zhu SL, Li N, Han YQ. Tracking control for switched nonlinear systems subject to output hysteresis via adaptive multi-dimensional Taylor network approach. *Int J Control*. 2023;96(7):1724-1735.
39. He WJ, Zhu SL, Li N, Han YQ. Adaptive finite-time control for switched nonlinear systems subject to multiple objective constraints via multi-dimensional Taylor network approach. *ISA Trans*. 2023;136:323-333.
40. Han YQ, He WJ, Li N, Zhu SL. Tracking control for large-scale switched nonlinear systems subject to asymmetric input saturation and output hysteresis: a new adaptive network-based approach. *Int J Robust Nonlinear Control*. 2022;32(14):8052-8072.
41. Lv WS, Wang F. Adaptive fuzzy finite-time control for uncertain nonlinear systems with asymmetric actuator backlash. *Int J Fuzzy Syst*. 2019;21(1):50-59.
42. Su H, Zhang WH. Finite-time tracking control for a class of MIMO nonstrict-feedback nonlinear systems via adaptive fuzzy method. *Int J Fuzzy Syst*. 2022;24(1):713-727.
43. Cui GZ, Xu SY, Zhang BY, Lu JW, Li Z, Zhang ZQ. Adaptive tracking control for uncertain switched stochastic nonlinear pure-feedback systems with unknown backlash-like hysteresis. *J Franklin Inst*. 2017;354(4):1801-1818.
44. He WJ, Han YQ, Li N, Zhu SL. Novel adaptive controller design for a class of switched nonlinear systems subject to input delay using multi-dimensional Taylor network. *Int J Adapt Control Signal Process*. 2022;36(3):607-624.
45. Ren BB, Ge SS, Tee KP, Lee TH. Adaptive neural control for output feedback nonlinear systems using a barrier lyapunov function. *IEEE Trans Neural Netw*. 2010;21(8):1339-1345.
46. Li HY, Wang LJ, Du HP, Boulkroune A. Adaptive fuzzy backstepping tracking control for strict-feedback systems with input delay. *IEEE Trans Fuzzy Syst*. 2017;25(3):642-652.
47. Zhang ZQ, Xie XJ. Asymptotic tracking control of uncertain nonlinear systems with unknown actuator nonlinearity and unknown gain signs. *Int J Control*. 2014;87(11):2294-2311.
48. Fu C, Wang QG, Yu JP, Lin C. Neural network-based finite-time command filtering control for switched nonlinear systems with backlash-like hysteresis. *IEEE Trans Neural Networks Learn Syst*. 2021;32(7):3268-3273.
49. Deng XF, Huang YQ, Wei LS. Adaptive fuzzy command filtered finite-time tracking control for uncertain nonlinear multi-agent systems with unknown input saturation and unknown control directions. *Mathematics*. 2022;10(24):46.
50. Du Y, Zhu SL, Zhai LL, Han YQ. Switching threshold-based event-triggered adaptive asymptotic tracking control for stochastic nonlinear systems with full-state constraints. *Int J Robust Nonlinear Control*. 2023;33(13):7908-7928.
51. Wei W, Zhang WH. Finite-time adaptive switched gain control for non-strict feedback nonlinear systems via nonlinear command filter. *Nonlinear Dyn*. 2020;100(4):3485-3496.
52. Zhu SL, Han YQ. Adaptive decentralized prescribed performance control for a class of large-scale nonlinear systems subject to nonsymmetric input saturations. *Neural Comput & Applic*. 2022;34(13):11123-11140.
53. Han YQ, Li N, He WJ, Zhu SL. Adaptive multi-dimensional Taylor network funnel control of a class of nonlinear systems with asymmetric input saturation. *Int J Adapt Control Signal Process*. 2021;35(5):713-726.
54. Wu JL. Stabilizing controllers design for switched nonlinear systems in strict-feedback form. *Automatica*. 2009;45(4):1092-1096.
55. Long LJ, Zhao J. Adaptive output-feedback neural control of switched uncertain nonlinear systems with average dwell time. *IEEE Trans Neural Networks Learn Syst*. 2015;26(7):1350-1362.
56. Yu JP, Zhao L, Yu HS, Dong WJ. Fuzzy finite-time command filtered control of nonlinear systems with input saturation. *IEEE Trans Cybern*. 2018;48(8):2378-2387.
57. Xie J, Yan SY, Yang D. DSC-based finite-time adaptive resilient control for a class of nonstrict-feedback switched nonlinear systems with deception attacks. *Int J Robust Nonlinear Control*. 2023;33(13):7851-7868.
58. Sharma M, Ward DG. Flight-path angle control via neuro-adaptive backstepping. Paper presented at: 2022 AIAA Guidance, Navigation, and Control Conference and Exhibit; August 05-08, 2002; Monterey, California.

How to cite this article: Zhao W, Han Y-Q, Zhou Y-F, Zhu S-L. Adaptive finite-time tracking control of nonlinear systems subject to input hysteresis and multiple objective constraints. *Int J Robust Nonlinear Control*. 2024;34(15):10292-10314. doi: 10.1002/rnc.7517